Optofluidic Intracavity Spectroscopic System for Single Biological Cell Identification

Hua (Linda) Shao

Advisor: Prof. Kevin L. Lear

Committee members: Prof. Carmen S. Menoni
Prof. V. Chandrasekar
Prof. Charles S. Henry

Department of Electrical and Computer Engineering
Colorado State University

October 31st, 2007

Colorado State University

Outline

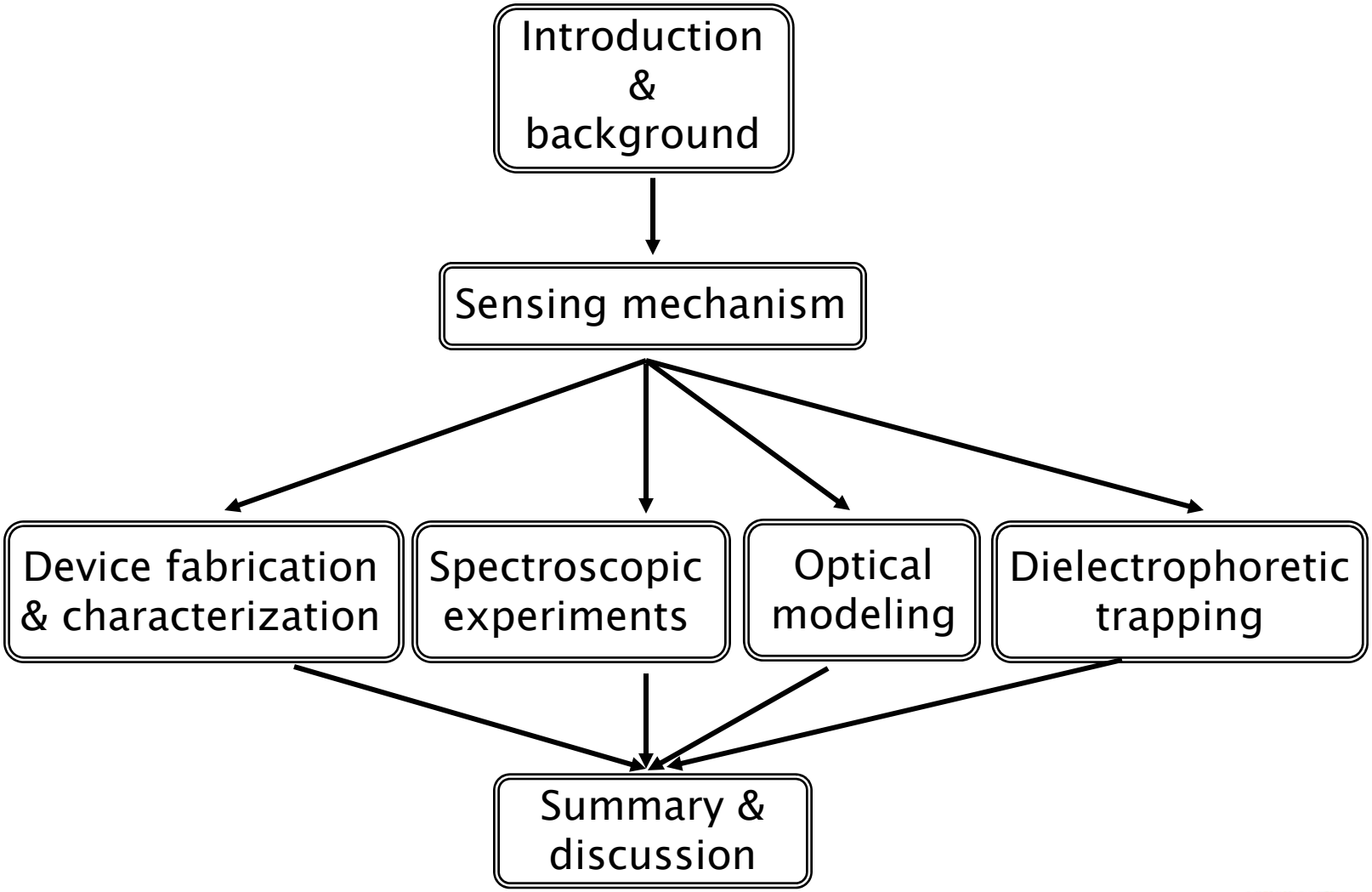

Outline

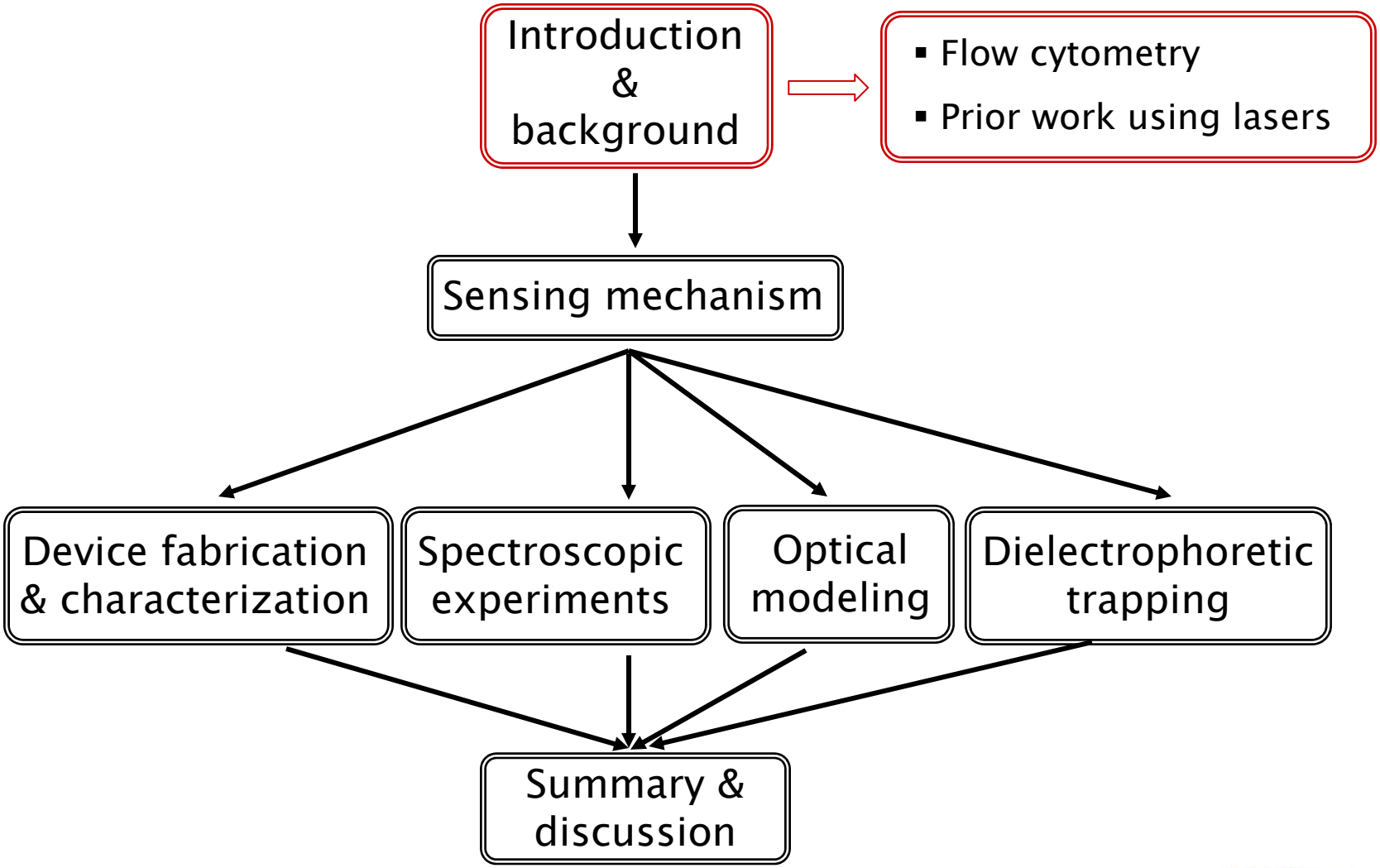

Motivation

Flow cytometer

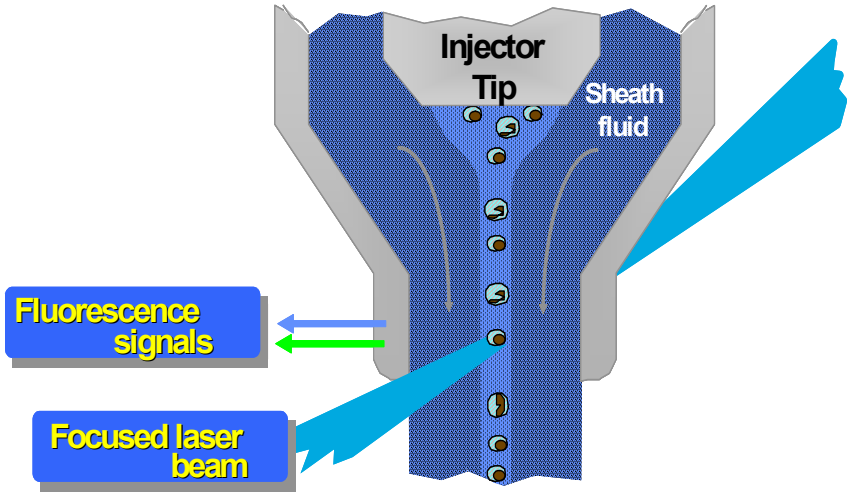

- Expensive ($200,000 ~ $500,000)
- Needs professional skills to operate

http://www.cyto.purdue.edu/flowcyt/theory.htm

Motivation

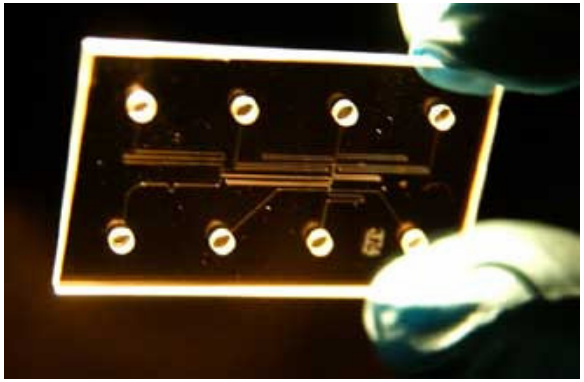

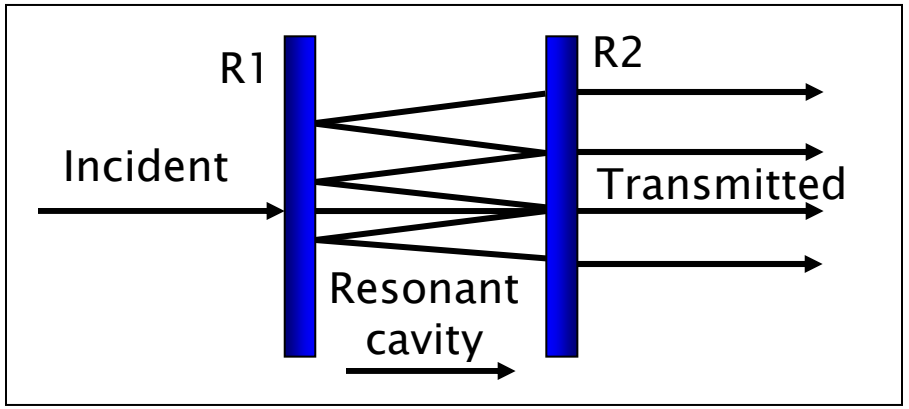

microfluidic chip

optical resonator

single cell identification

- Low cost
- Lab-on-chip
- Label-free
- Easy to operate

- Drug screening
- Clinical diagnosis
- Environment monitoring
- Homeland security

Prior work–optically pumped laser based biosensor

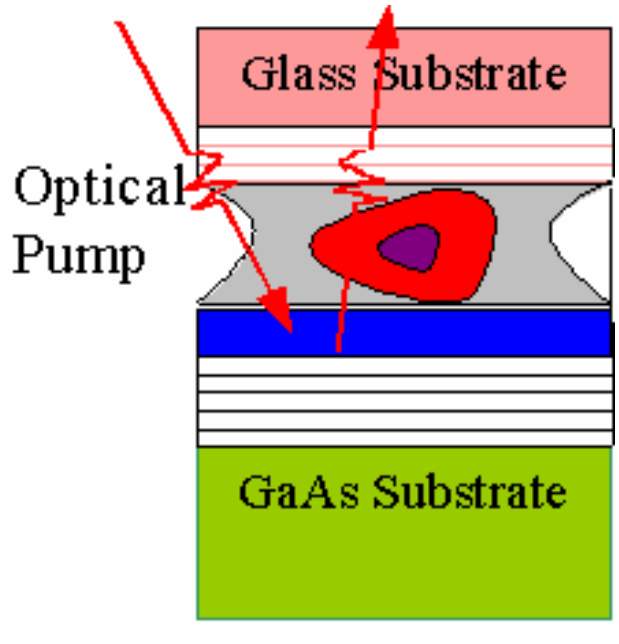

P. L. Gourley, Sandia National Lab, 1997.

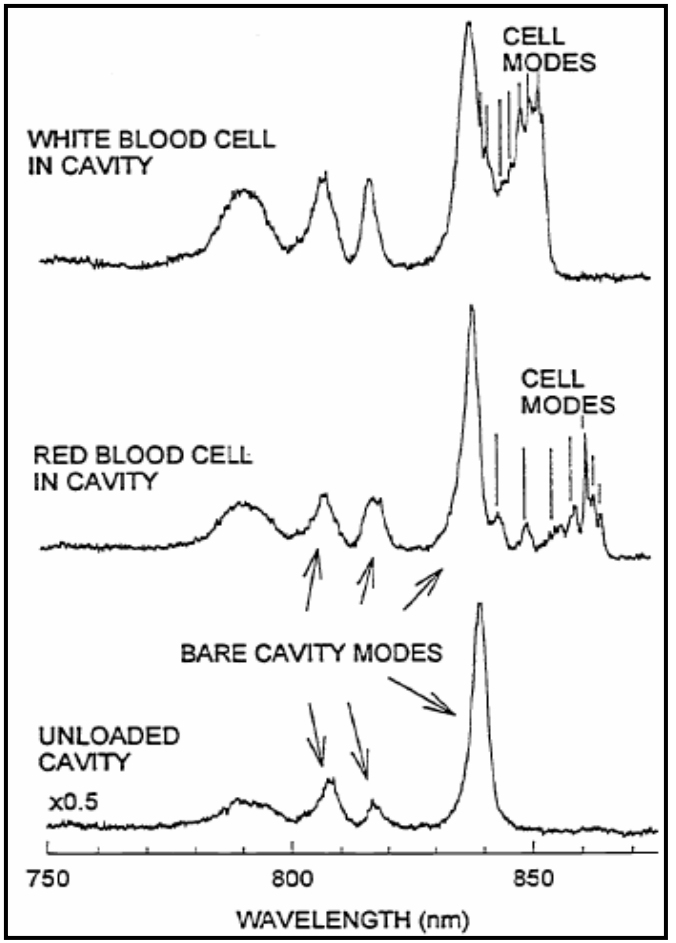

Prior work–electrically injected laser based biosensor

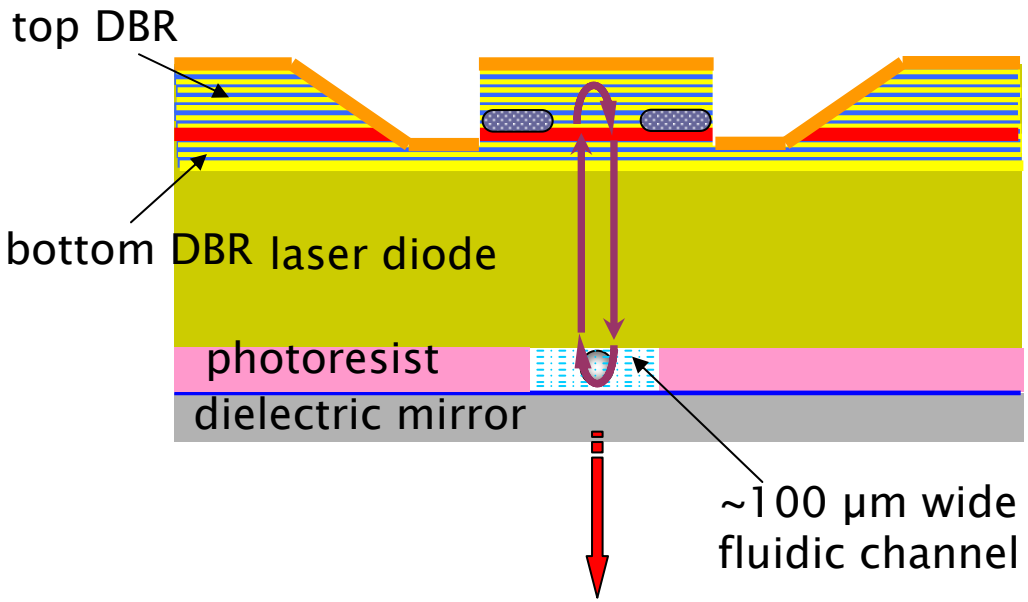

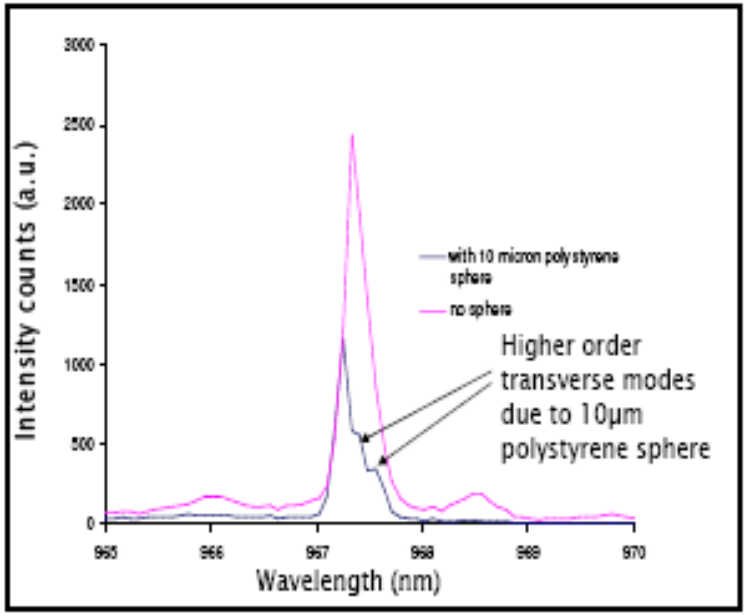

Dhiraj Kumar, CSU, 980 nm bottom-emitting design (2002-2005)

Outline

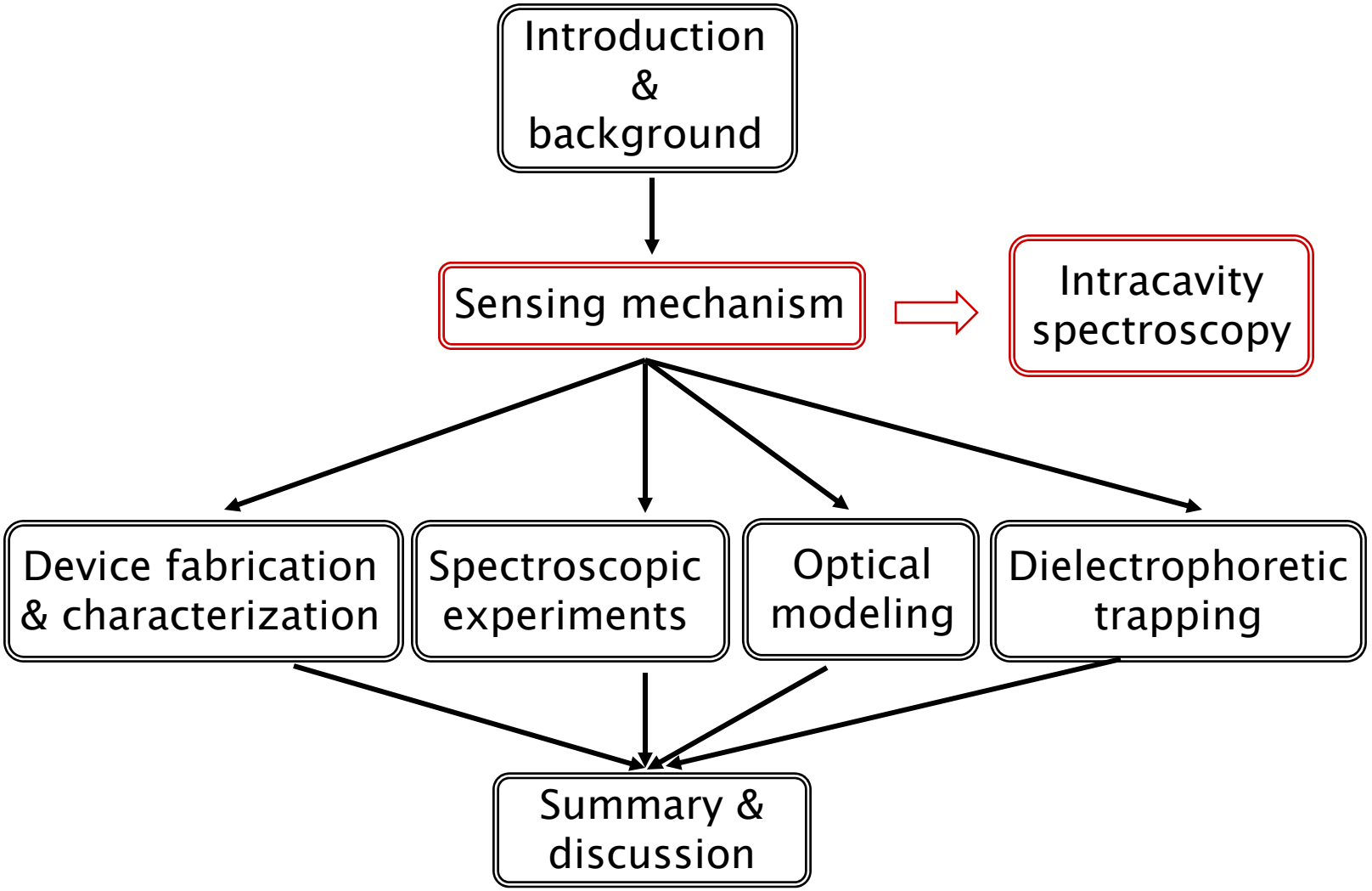

Optofluidic intracavity spectroscopy (OFIS)

1) no sphere

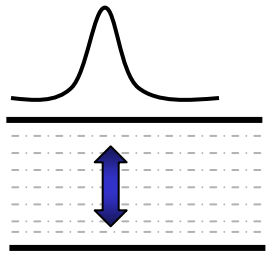

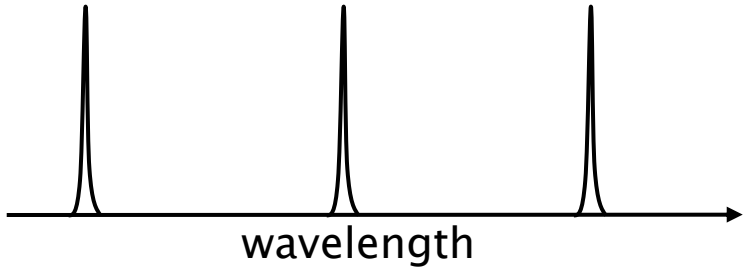

2) small cell

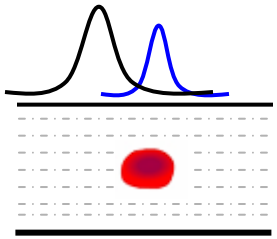

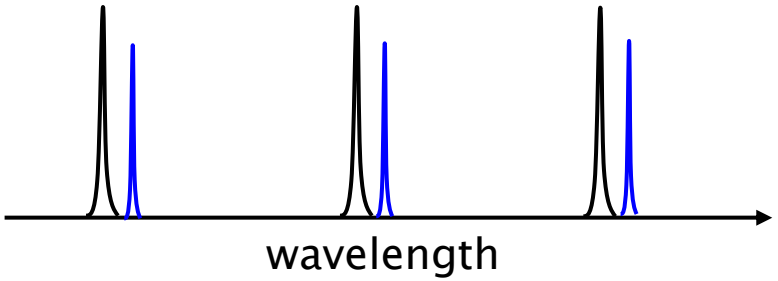

3) large cell

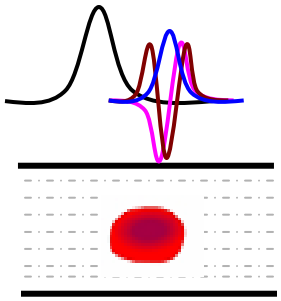

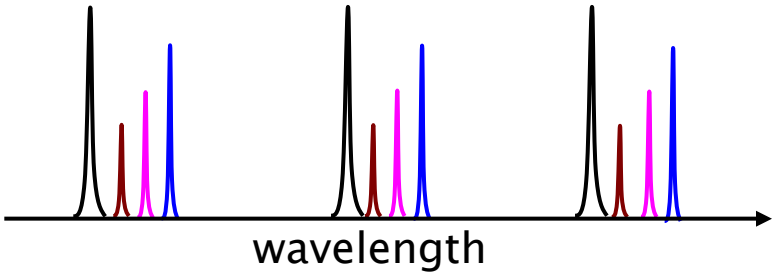

Transmission spectrum is modified by the cell phenotype.

Passive cavity OFIS

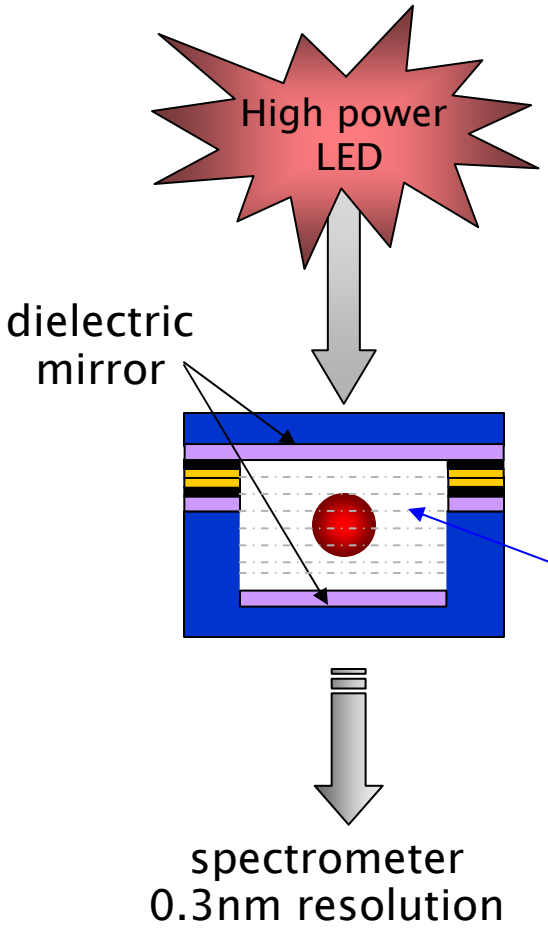

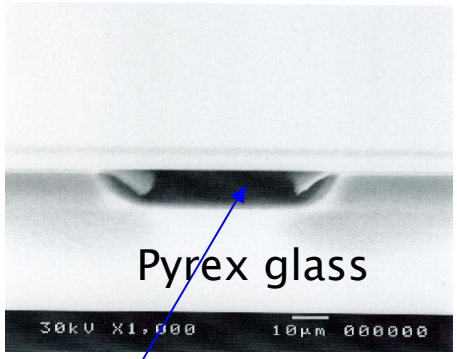

fluidic channel

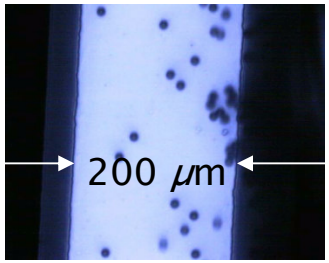

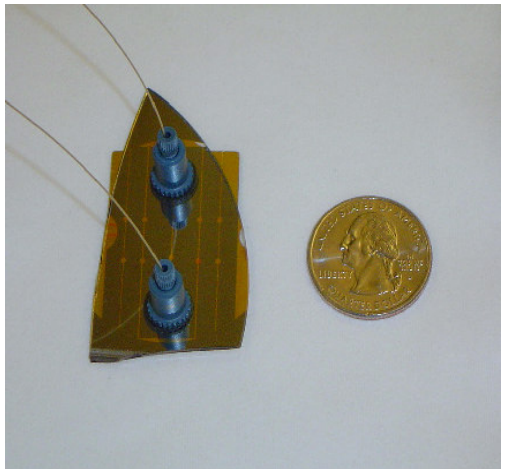

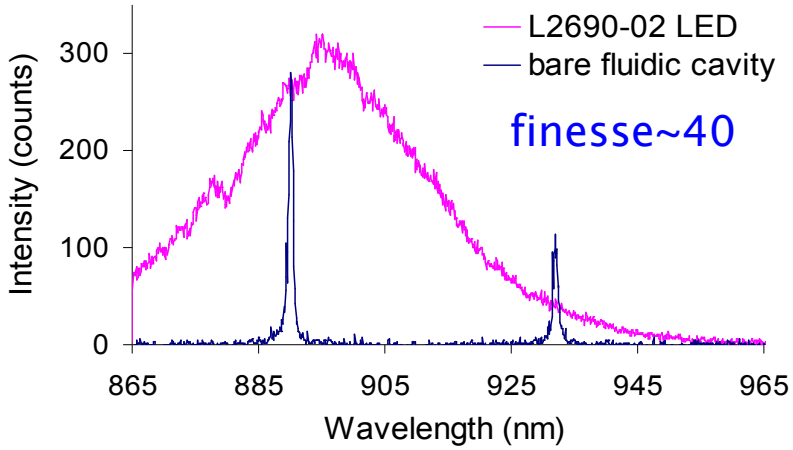

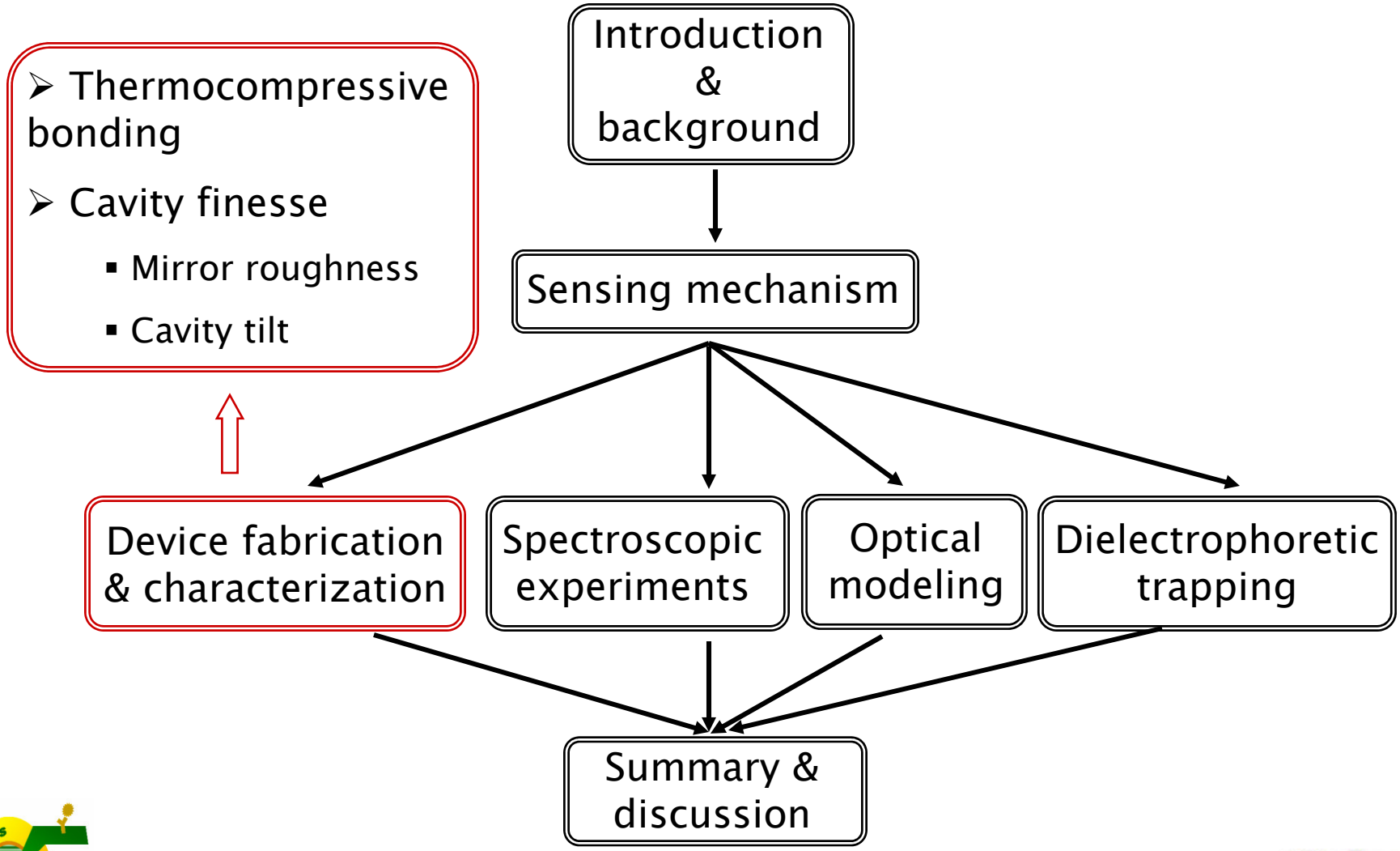

Gold coated cavity fabrication

Gold coated cavity fabrication

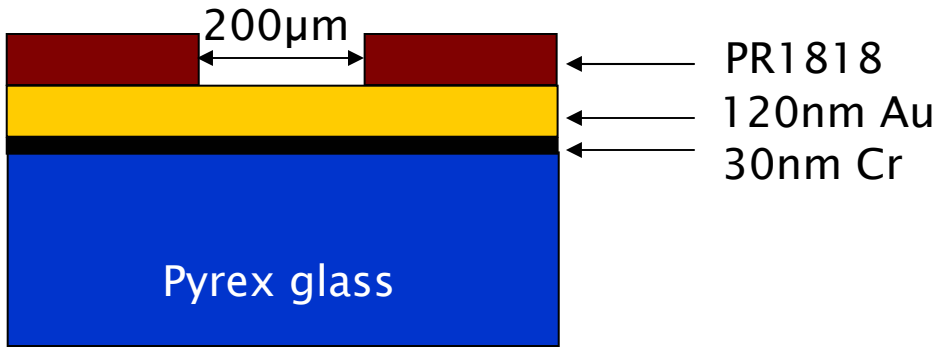

Gold coated cavity fabrication

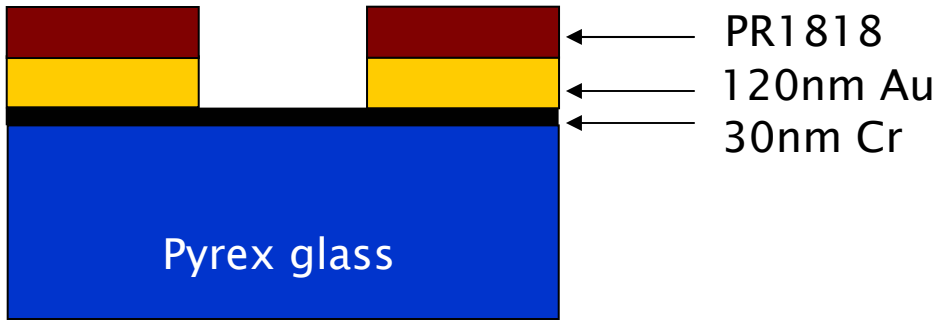

Gold coated cavity fabrication

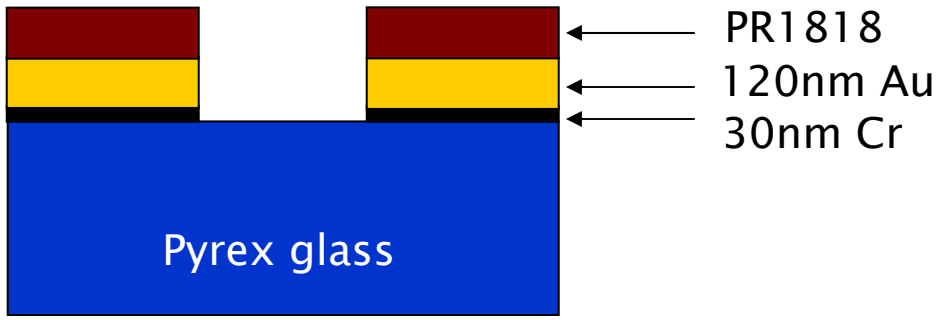

Gold coated cavity fabrication

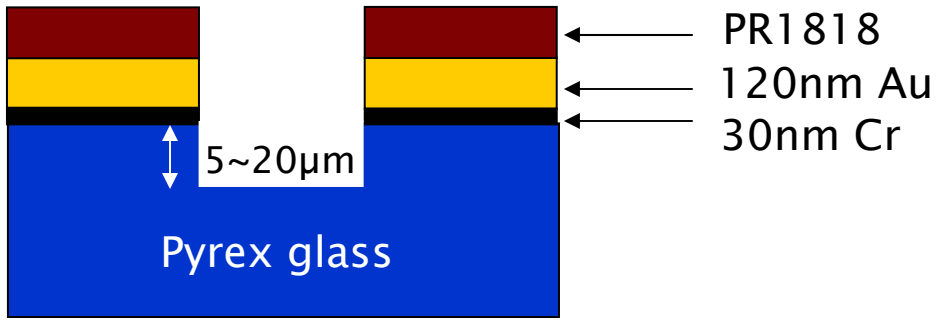

Device fabrication-glass etching

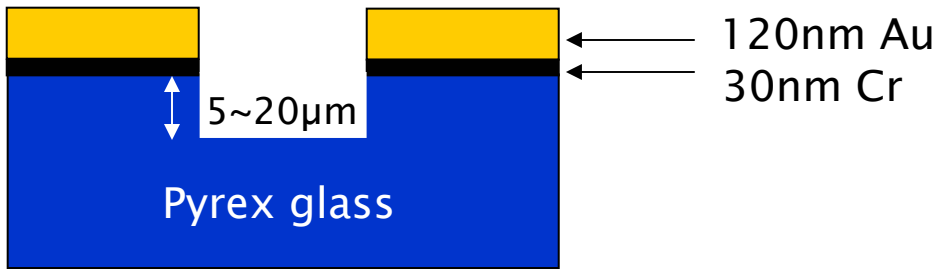

Gold coated cavity fabrication

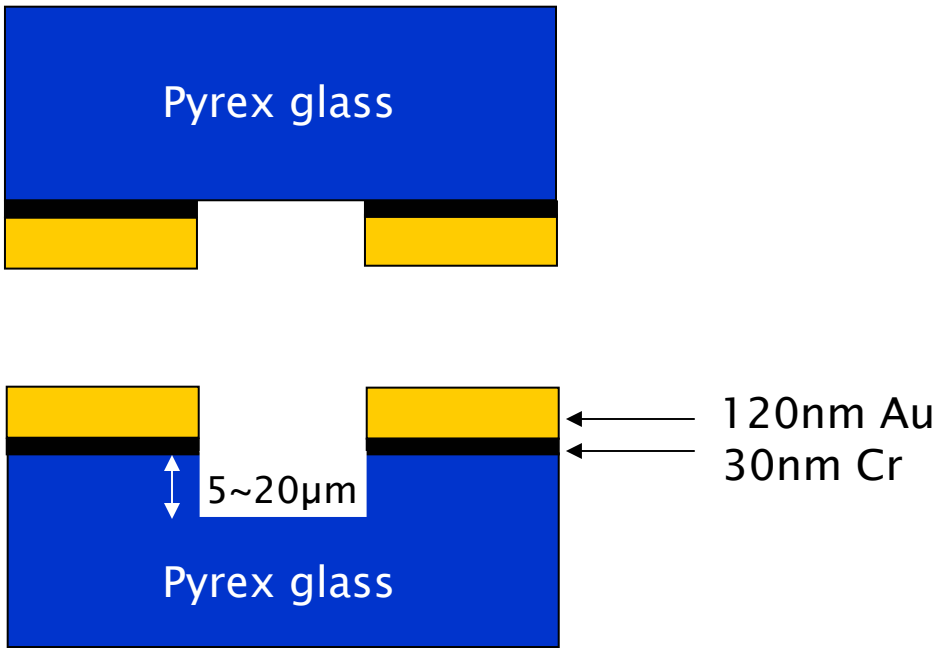

Gold coated cavity fabrication

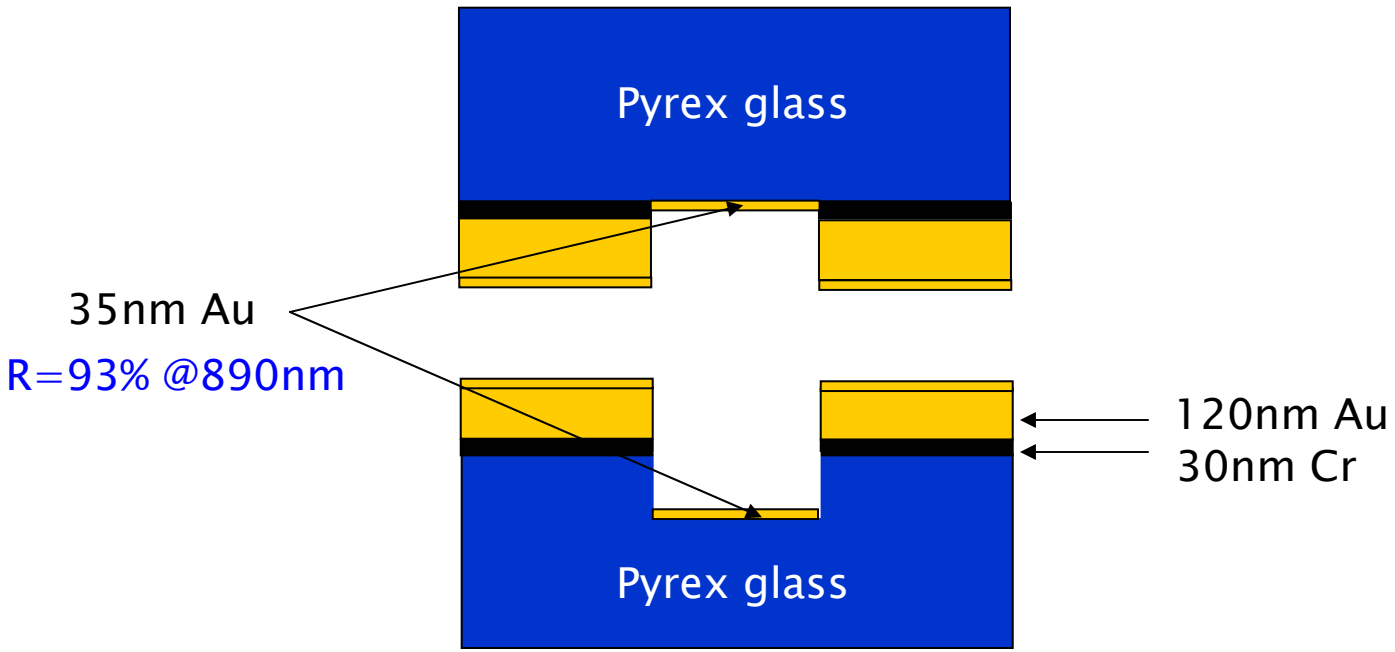

Device fabrication–wafer bonding

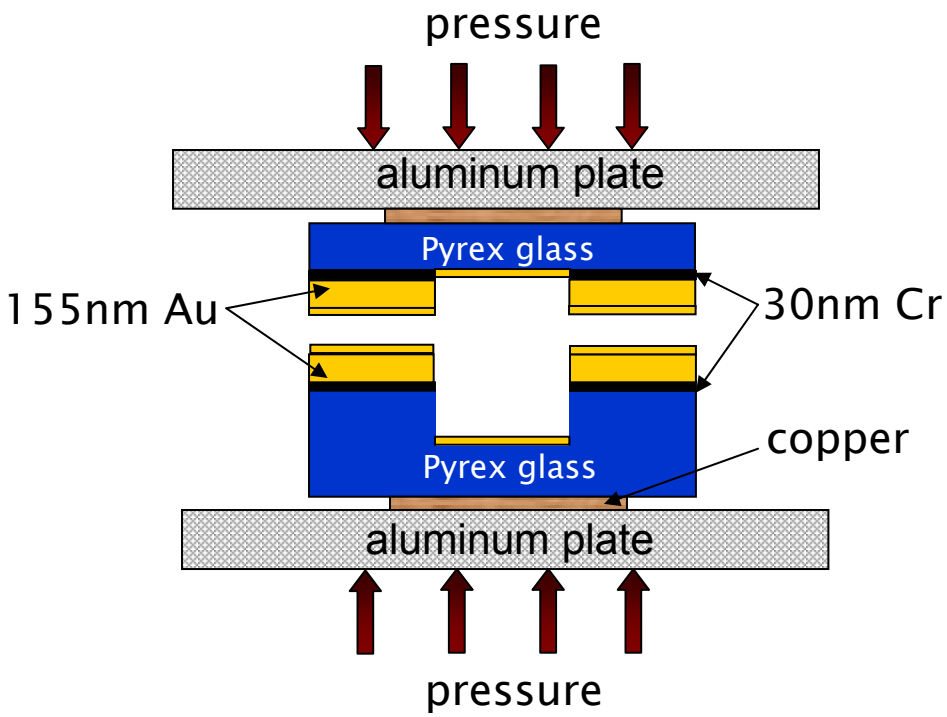

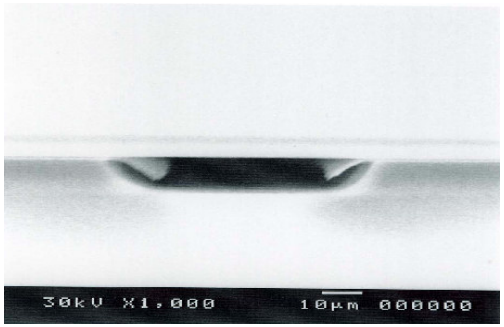

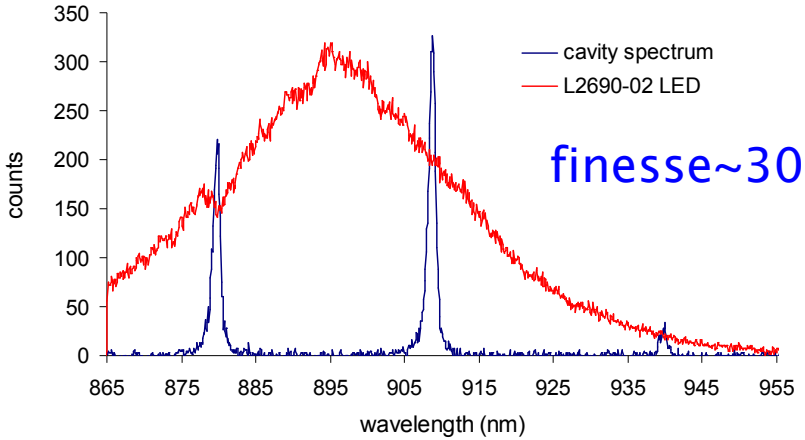

Thermocompressive gold-to-gold diffusion bonding at 350^0C in a 10^{-3} torr vacuum.

Cavity finesse characterization

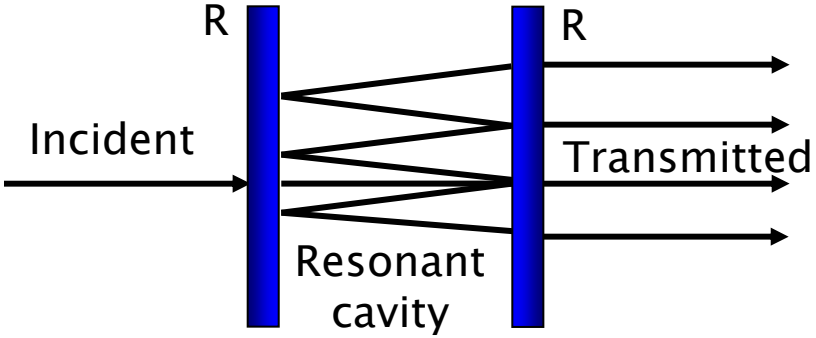

For R=93% reflective gold mirrors

$$F_{ideal} = \frac{\pi\sqrt{R}}{1-R} = 43.3$$

$$F_{measured} = FSR / FWHM = 30$$

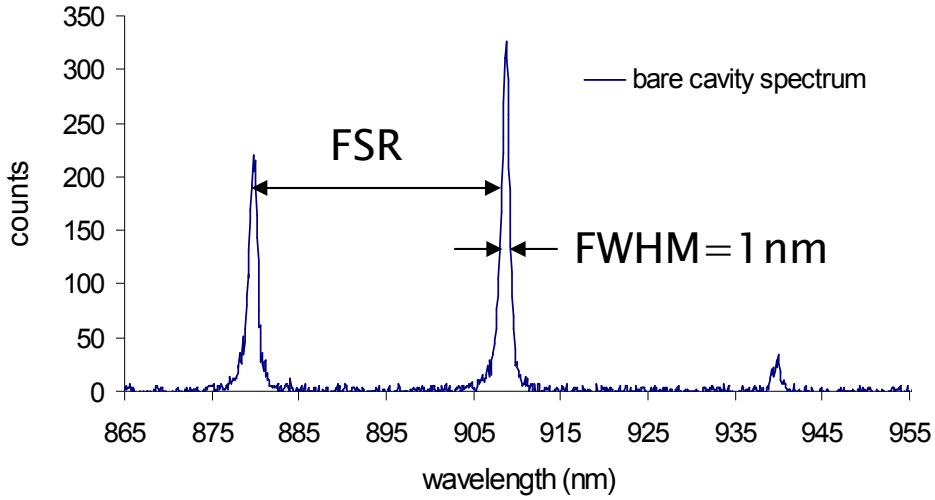

- Surface roughness (reflectivity decrease)
- Mirror tilt (cavity length variation)

Finesse vs. mirror roughness

Atomic force microscopy

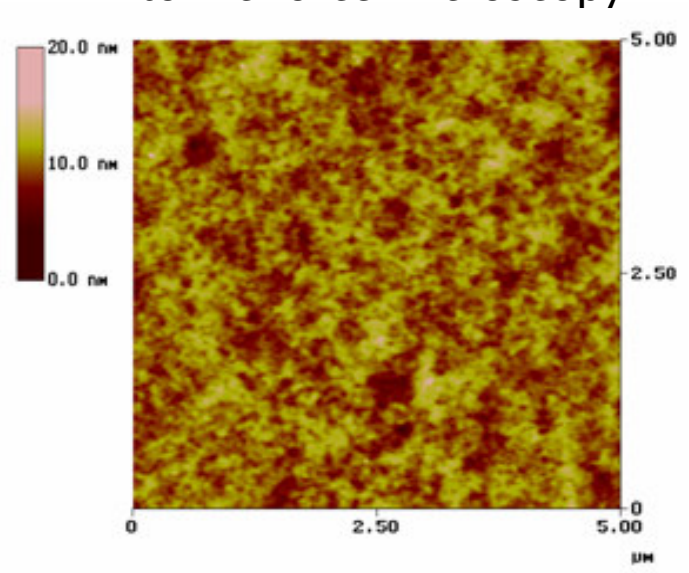

RMS roughness=1.309nm
(before gold coating)

=1.765nm
(after gold coating)

Cavity finesse with surface roughness:

$$\frac{1}{F_{total}^2} = \frac{1}{F_{ideal}^2} + \frac{1}{F_{sr}^2} + \frac{1}{F_{tilt}^2}$$

$$F_{sr} = \frac{\pi}{\sqrt{3}\sigma_r} = \frac{\pi}{\sqrt{3}(2\pi/\lambda)RMS_{roughness}}$$

Cavity finesse is reduced by 4.2% due to a RMS roughness of 1.765nm.

G. J. Sloggett, "Fringe broadening in Fabry-Perot interferometers", *Appl. Opt.*, 23 (14), 2427, 1984.

Cavity depth measurement

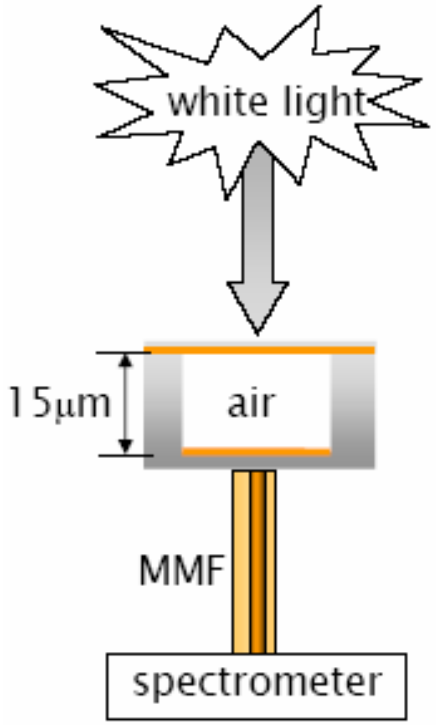

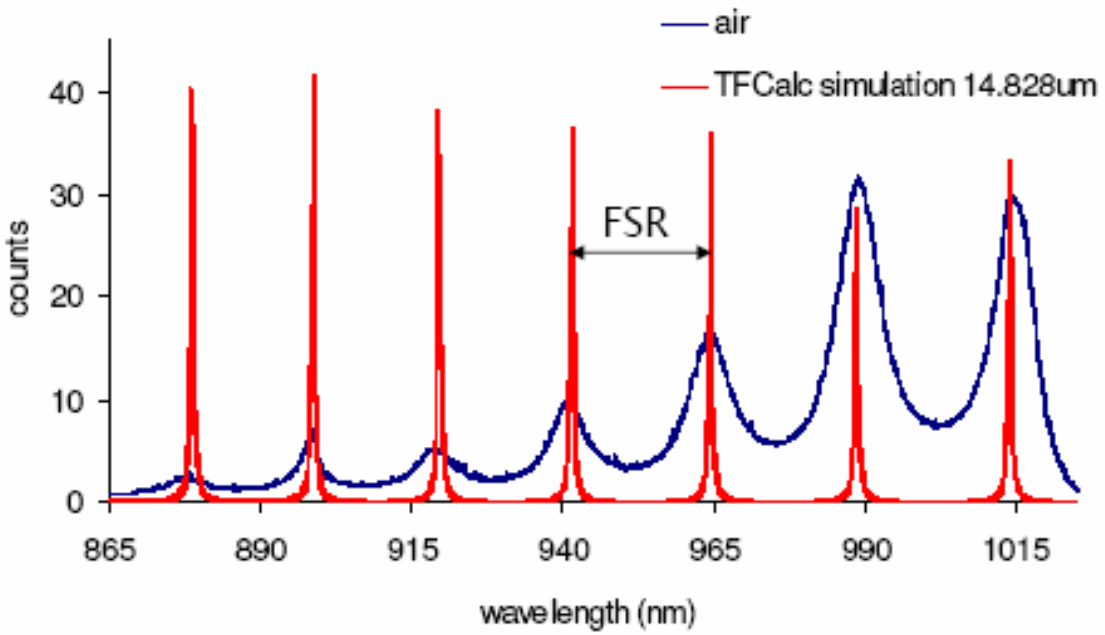

$$L_{cav} = \frac{\lambda^2}{2 n_{cav} FSR}$$

Finesse vs. cavity mirror tilt

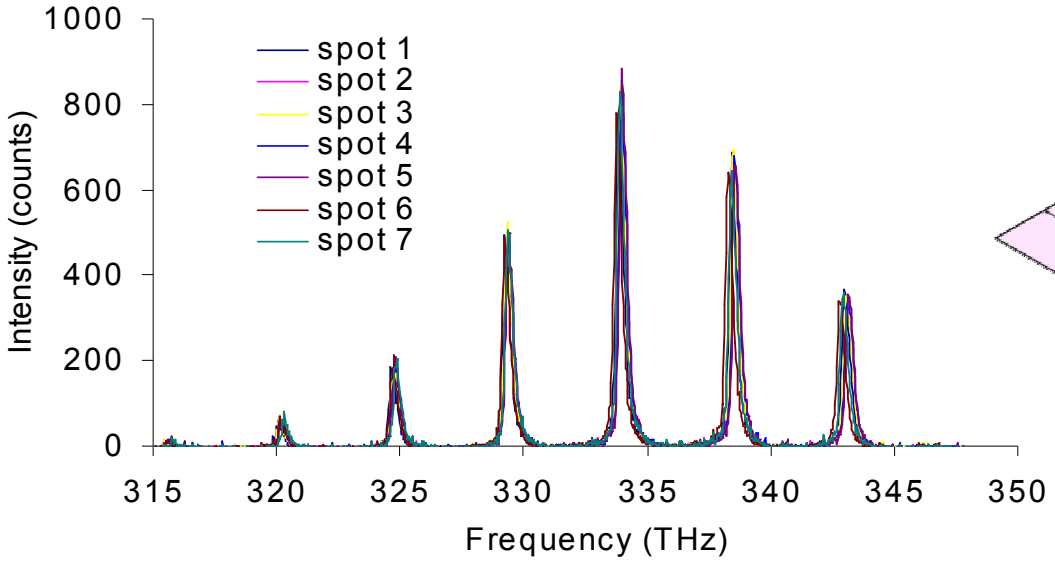

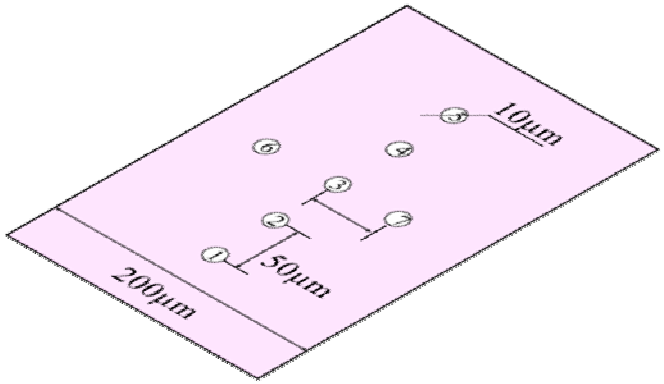

Direction	Tilt angle	F_{tilt}	F_{total}
Along channel	0.095^0	46.60	35.71
Across channel	0.053^0	83.53	38.42

$$F_{tilt} = \frac{\sqrt{3}}{\pi\sigma_{tilt}} = \frac{\sqrt{3}}{\pi\left[k_0 n (D/2)\tan(\Gamma_{tilt})\right]}$$

$$F_{total} = \sqrt{F_{ideal}^{-2} + F_{sr}^{-2} + F_{tilt}^{-2}} = 30.99$$

G. J. Sloggett, "Fringe broadening in Fabry-Perot interferometers", *Appl. Opt.*, 23 (14), 2427, 1984.

2nd generation device with dielectric mirrors

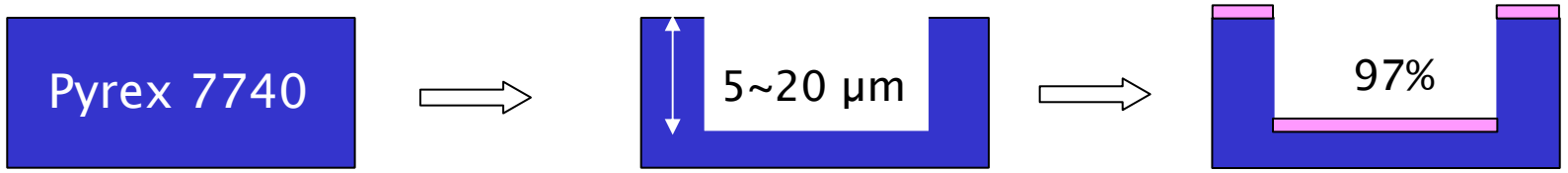

(a) Pyrex wet etching

(b) 13 layer HfO_2/SiO_2 dielectric mirror

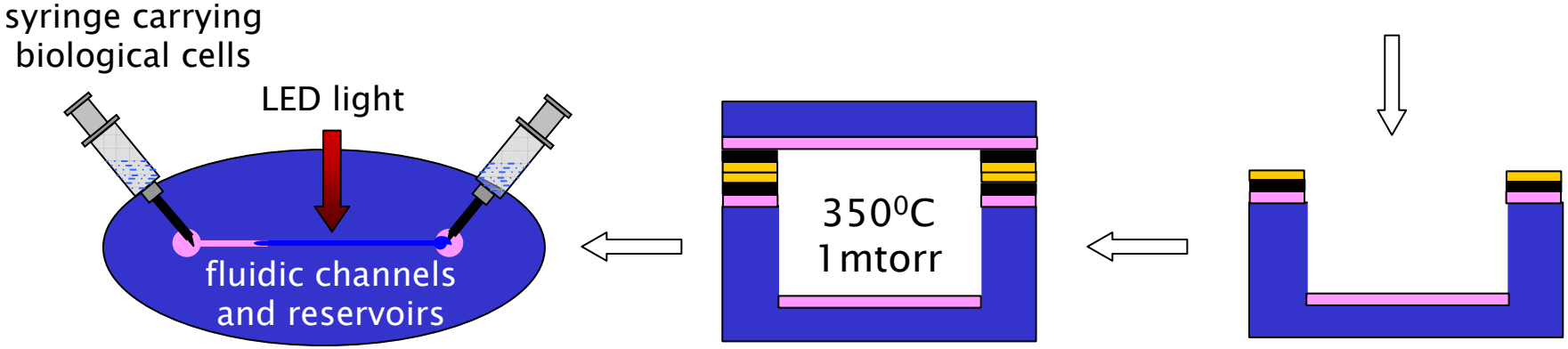

(f) Nanoport assembly integration

(d) thermocompressive bonding

(c) Cr/Au deposition (lift-off)

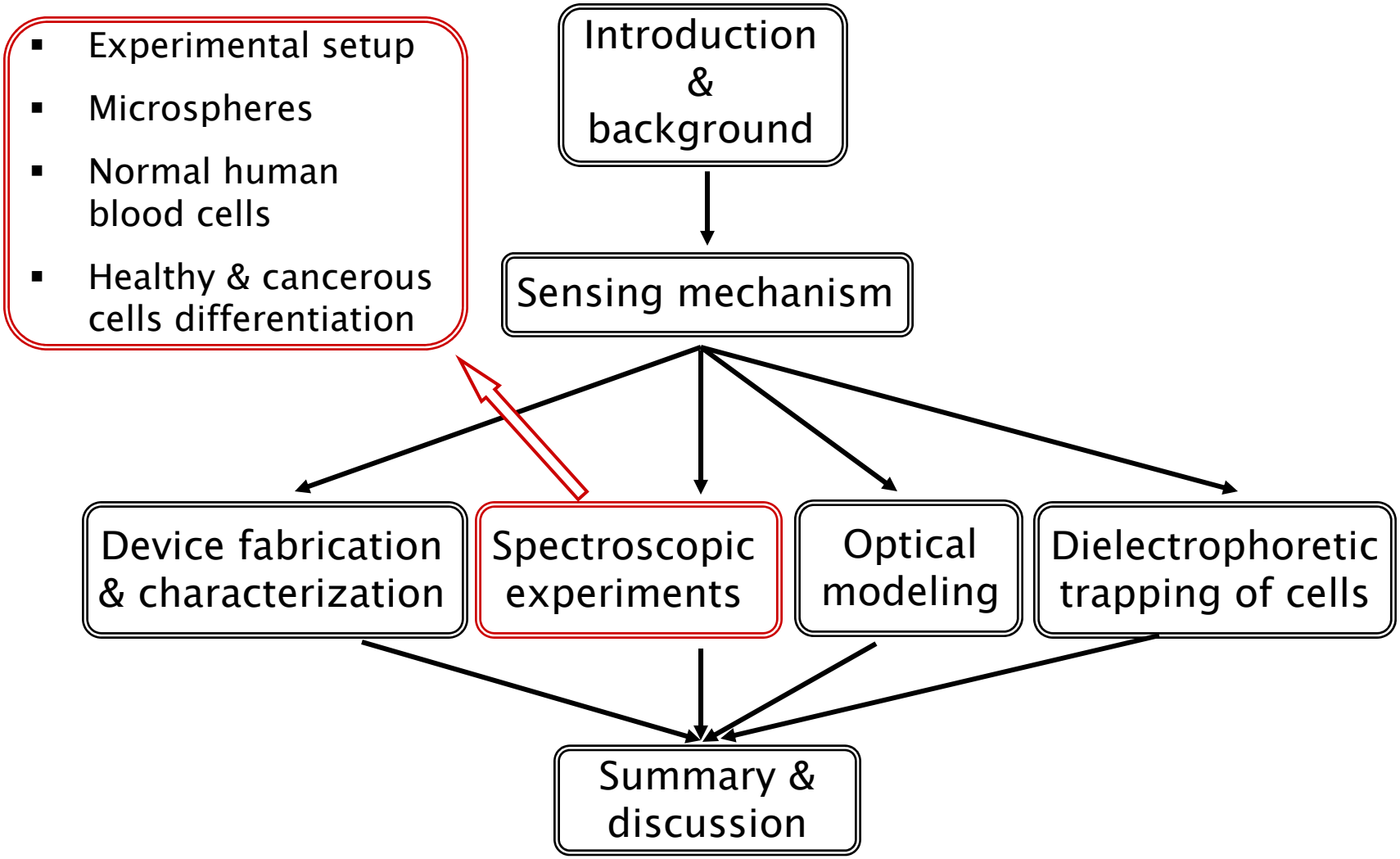

Experimental setup

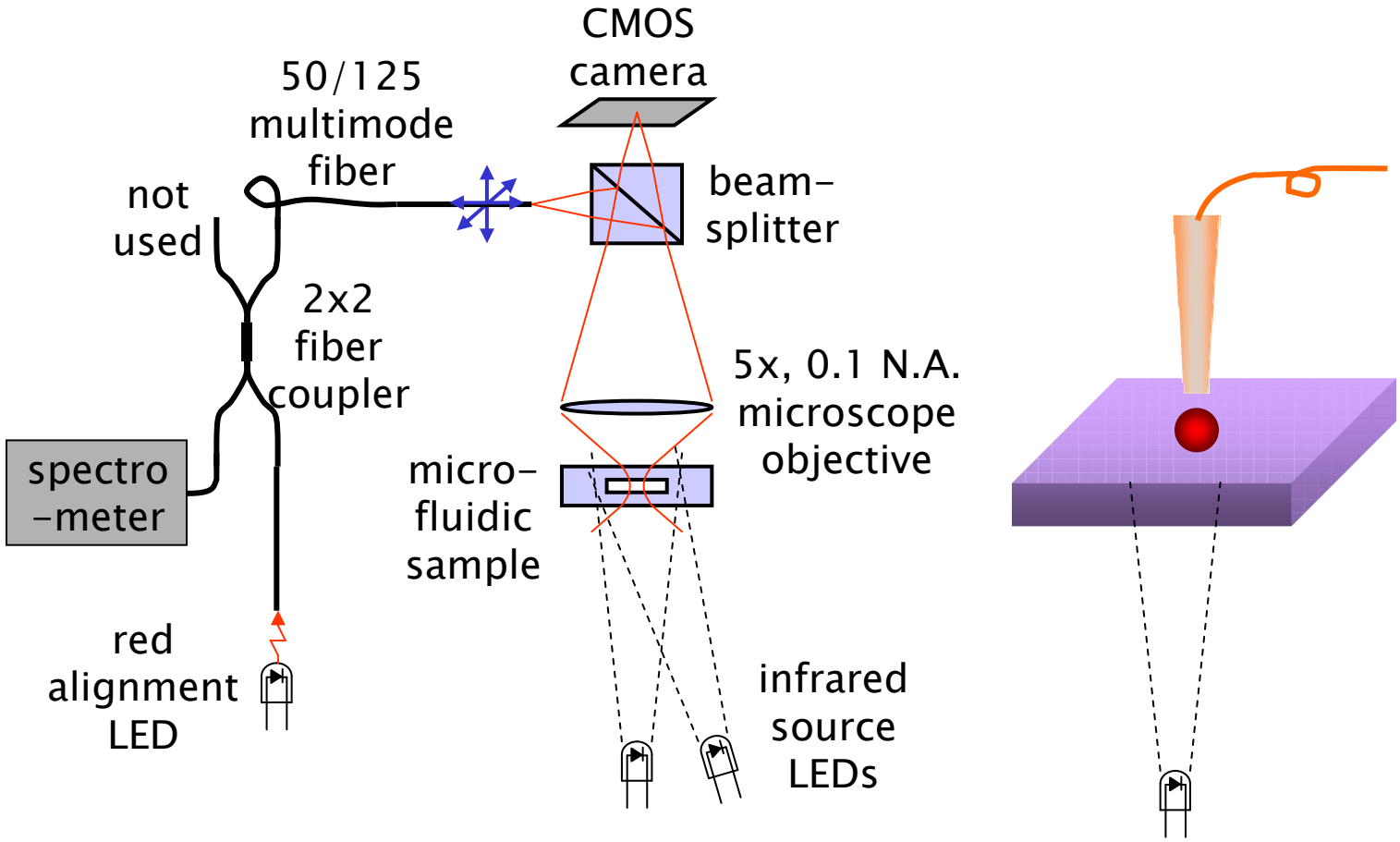

Experimental spectra of standard polystyrene microspheres (n=1.59)

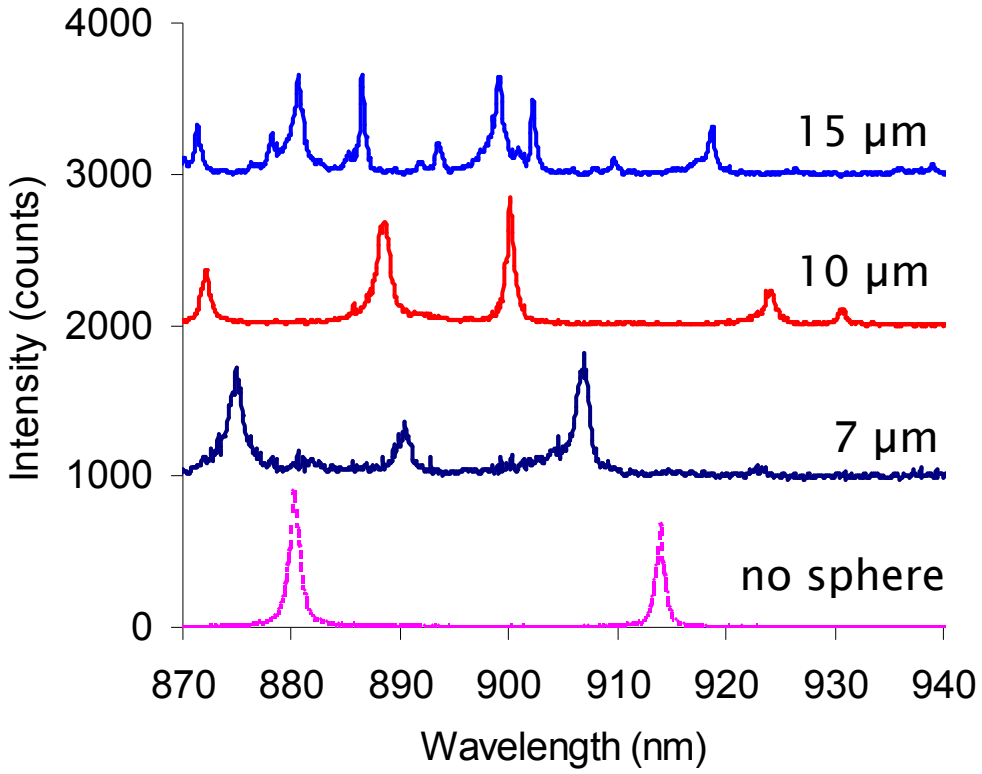

- Smaller spheres have larger transverse mode spacing than larger spheres.
- Measured spectral repeatability of polystyrene spheres were not good due to ±3% size variations (Bangs Laboratories, Inc.).

Transmission spectra of single yeast cells

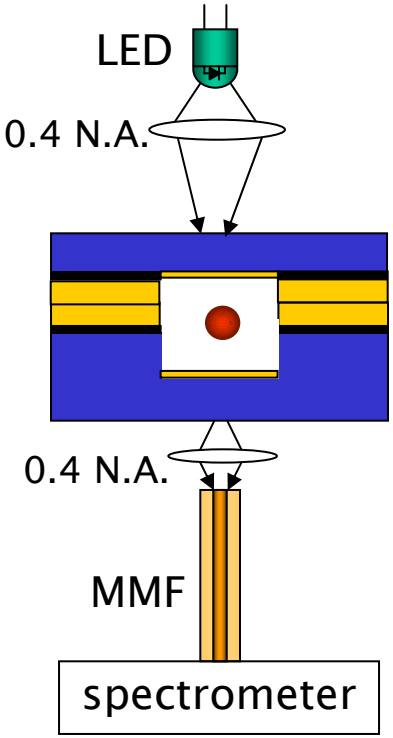

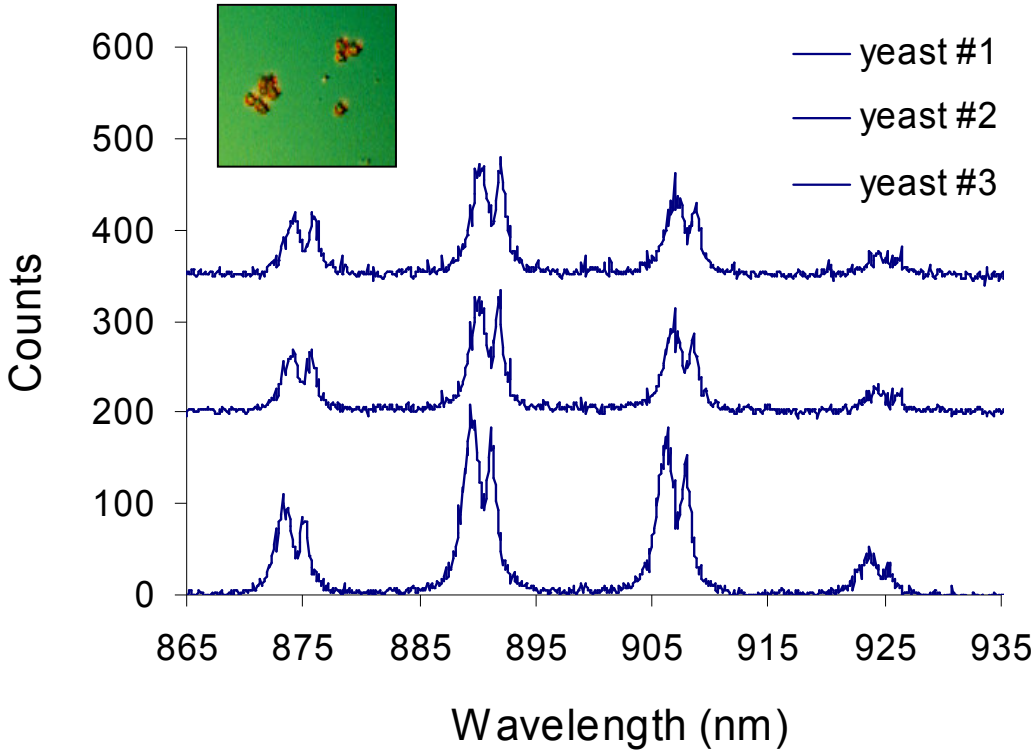

Yeast cells are globose to ovoid in shape and approximately 8~15 μm in diameter.

Human blood cells

red blood cells
(T:0.81~2.58μm, D:7-20μm)

white blood cells (7~20μm)

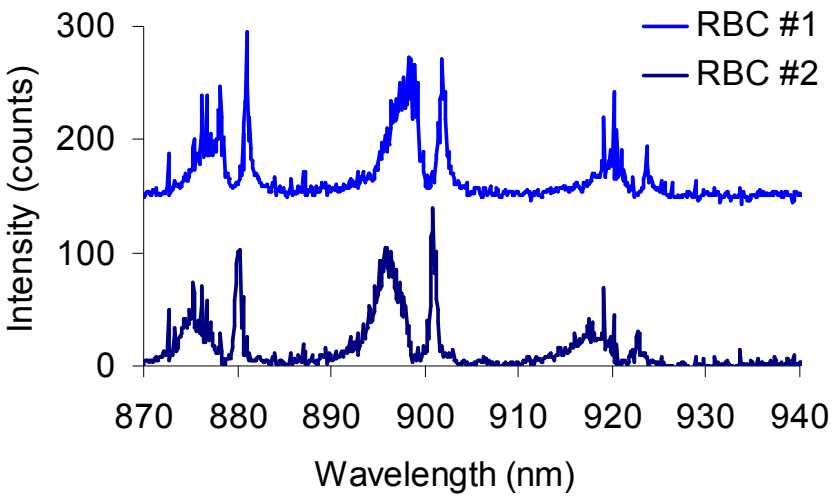

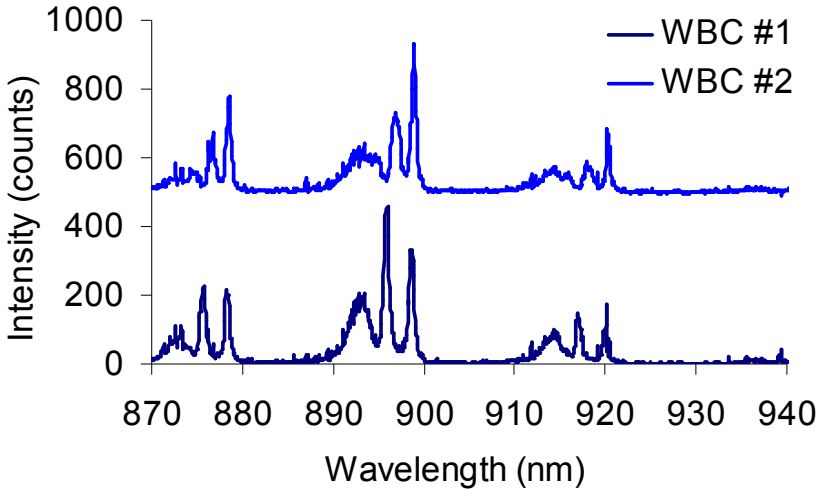

Distinctive transmission spectral properties, including number of modes and mode shape, have been observed on two different types of blood cells.

Canine lymphoma vs. PBMCs

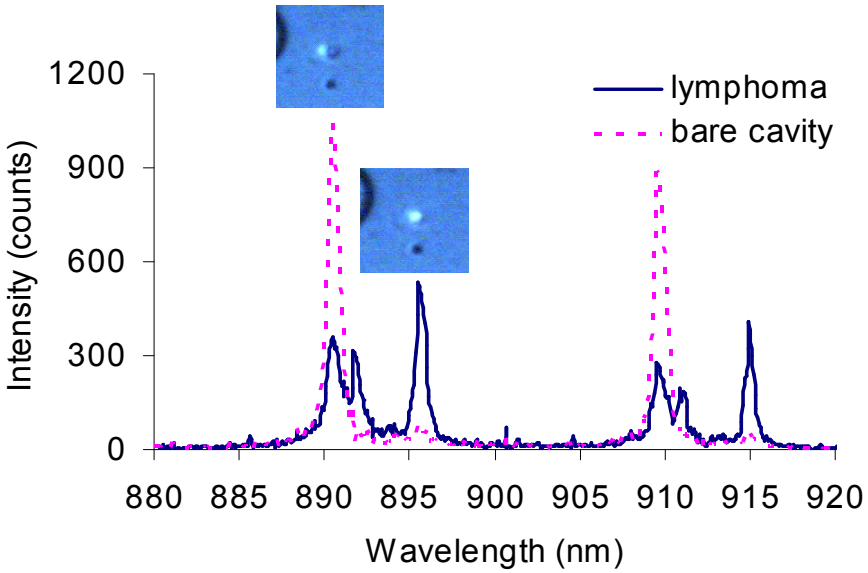

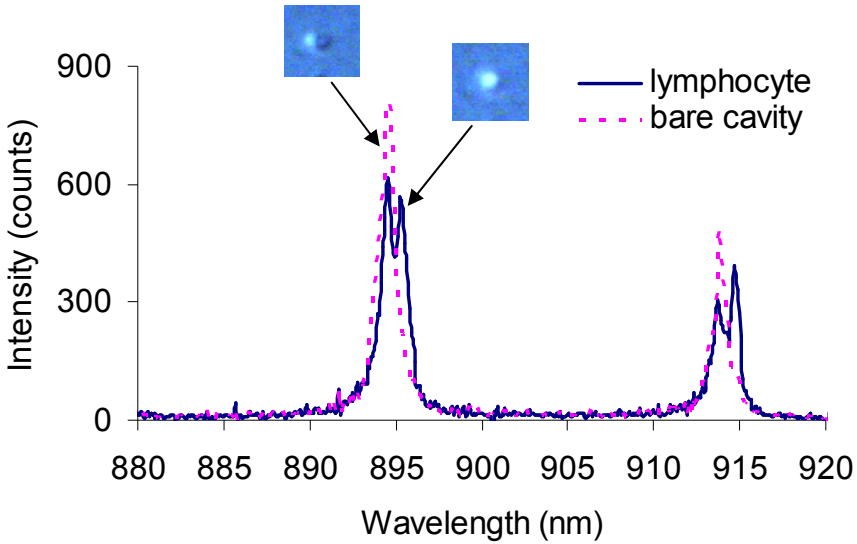

- Cancerous cells have larger nuclei than normal cells. Therefore higher refractive indices.
- Canine lymphoma grown from the cell lines are more homogeneous than the baseline peripheral blood mononuclear cells (PBMCs).

Cell spectral repeatability

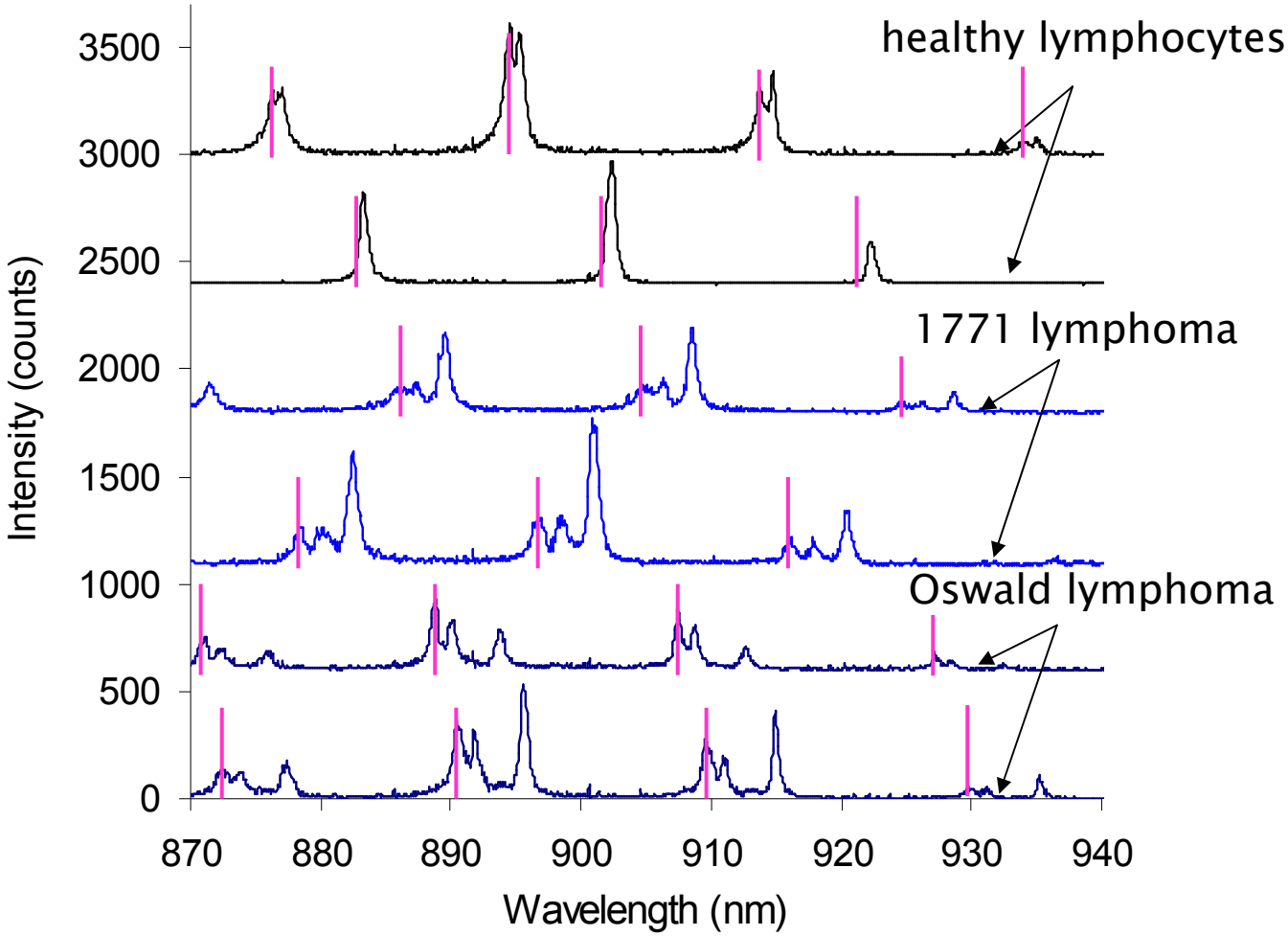

Cellular mode determination

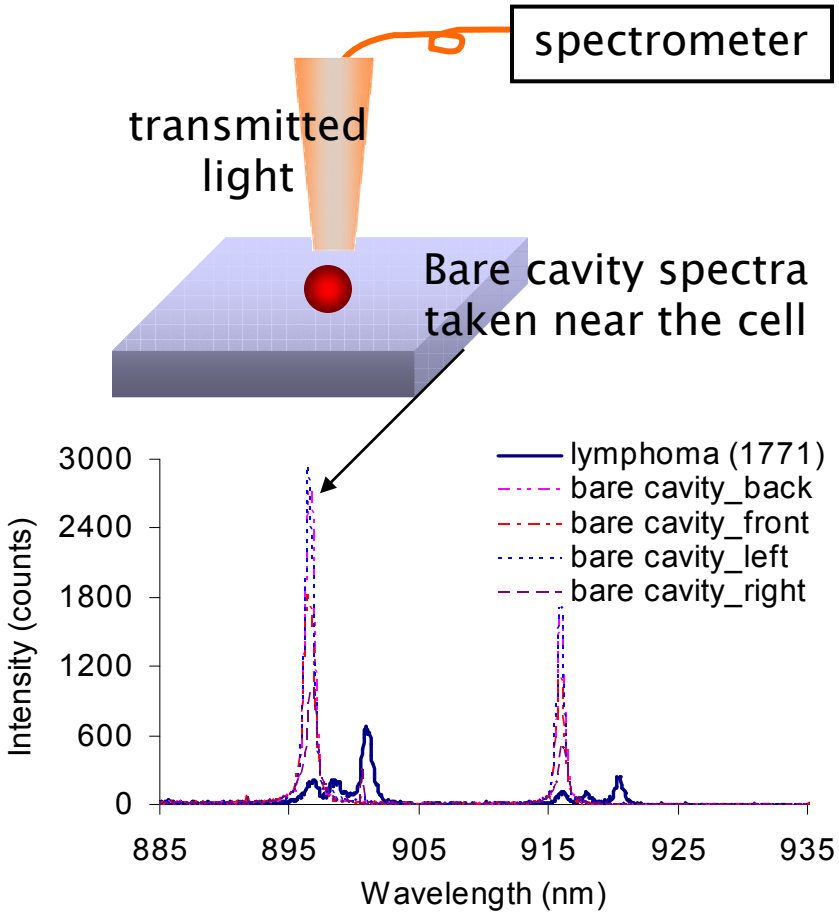

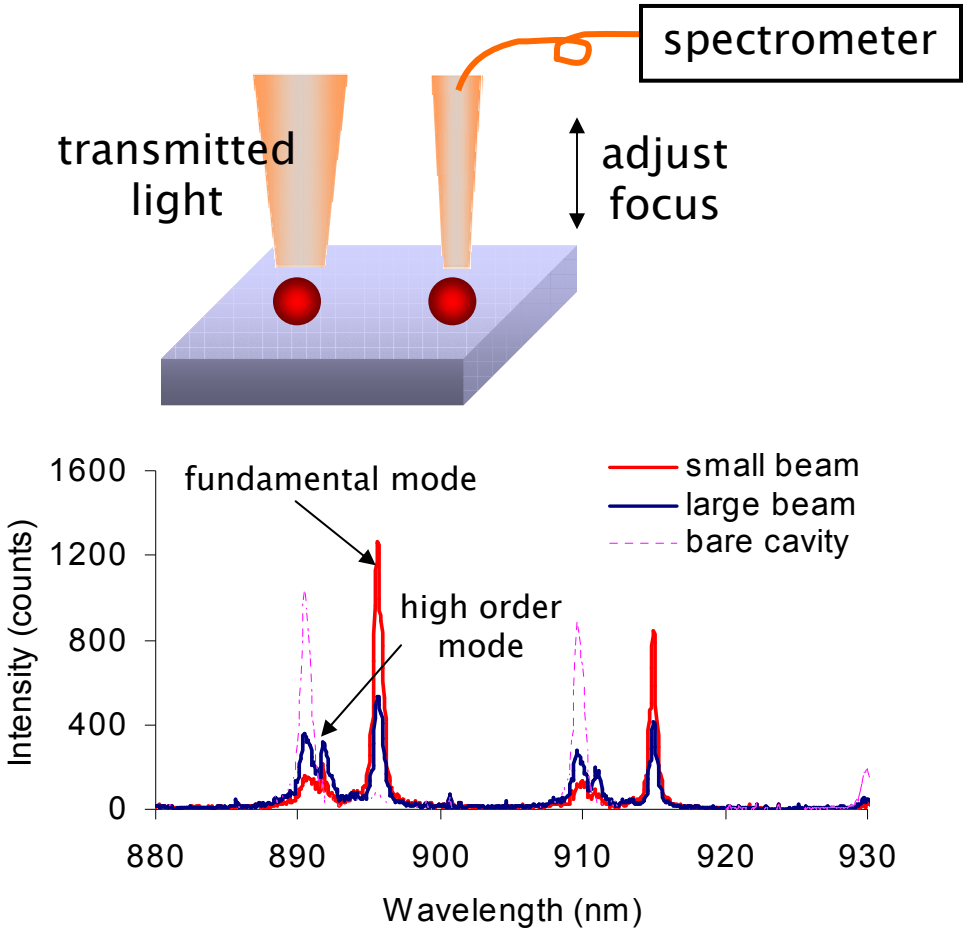

- Bare cavity mode is on the short wavelength side.
- Fundamental mode is more likely to be induced by the nucleus due to the greater overlap with the nucleus.

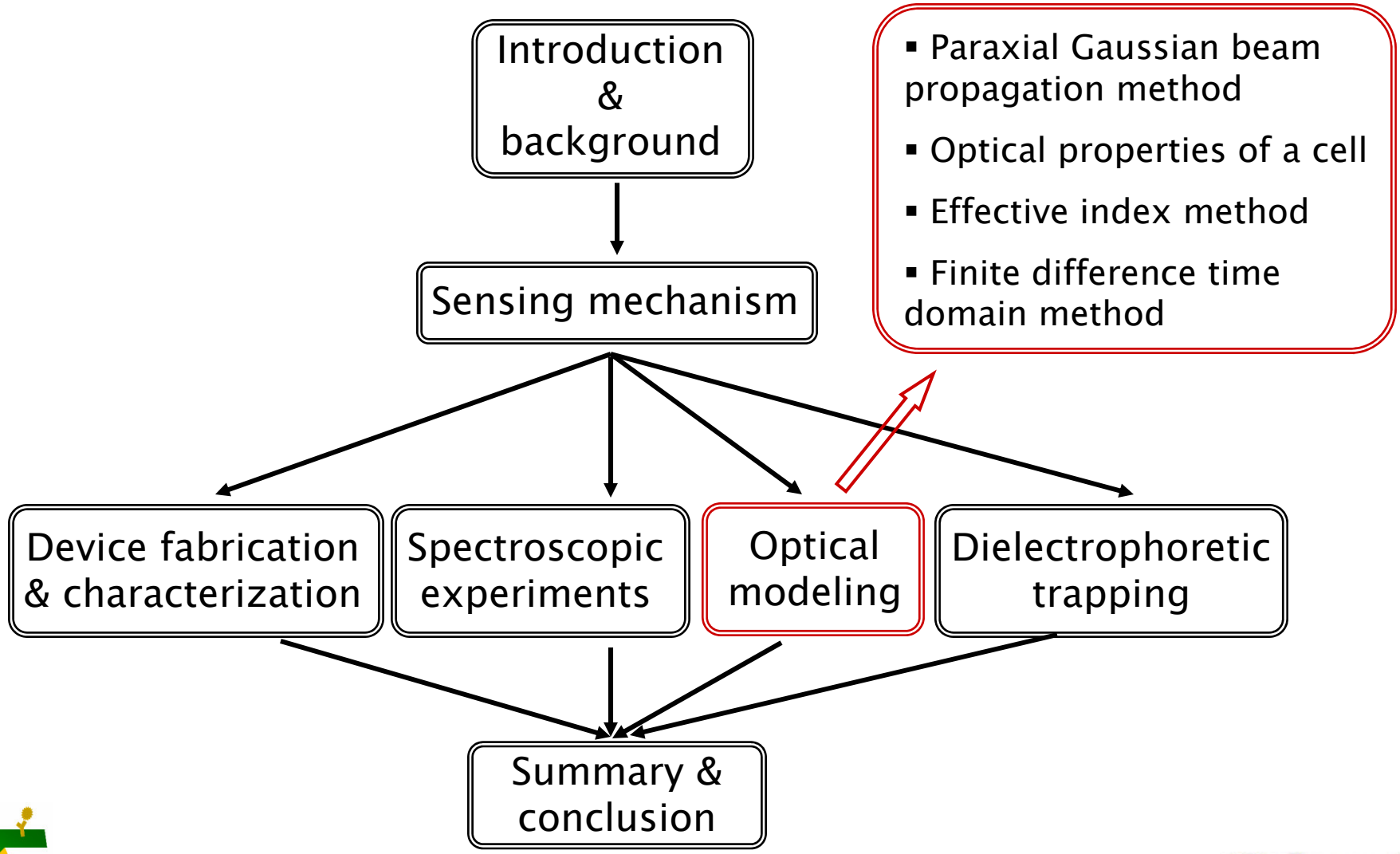

Cavity stability analysis

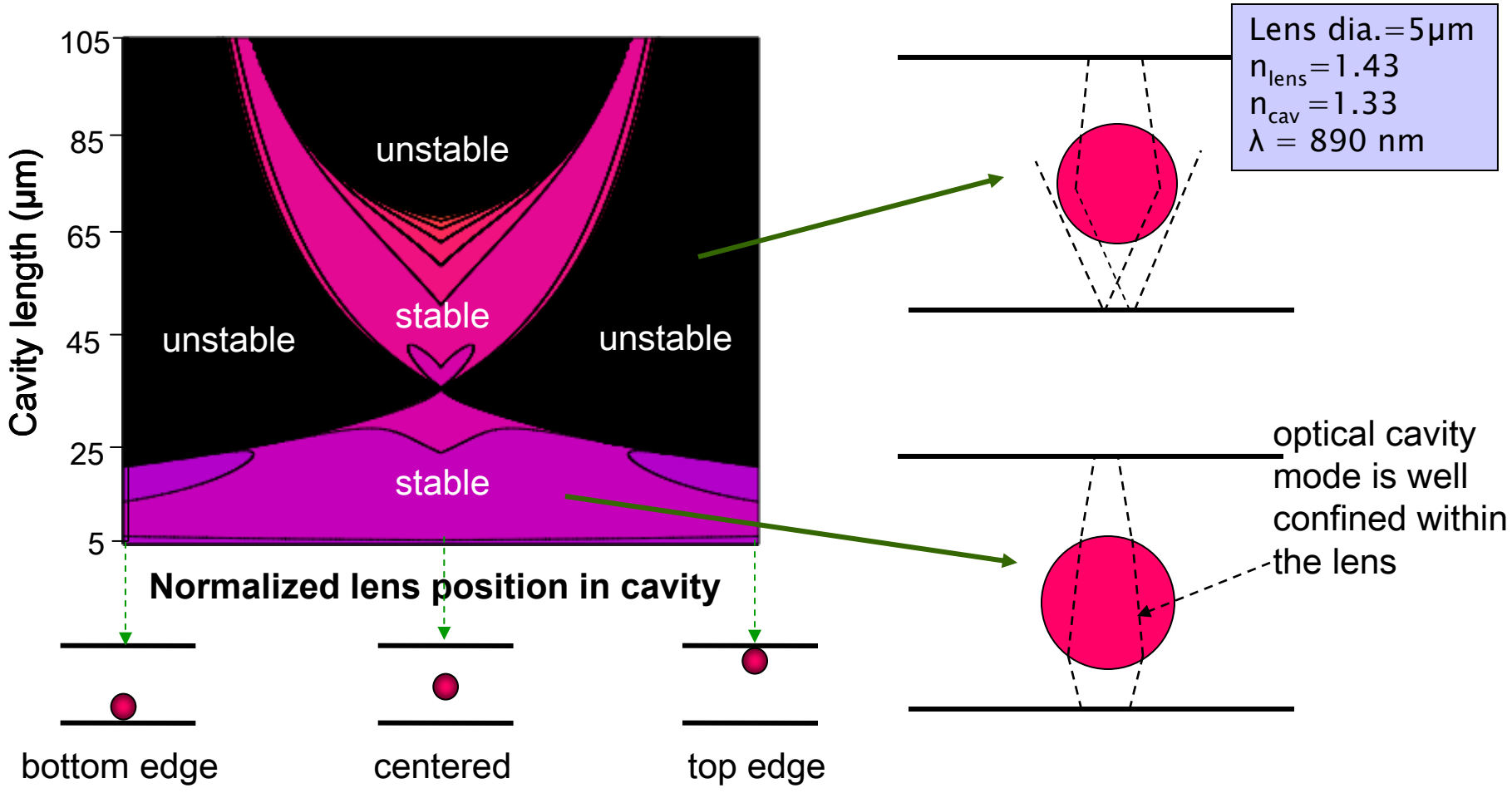

Cavity length should be minimized in order to provide stable resonator operation for cell positions throughout the resonator.

Transverse mode spacing

- Mode spacing is signature for sphere size and refractive index
- Mode spacing changes with lens position in cavity
- Short cavity length minimizes the variation in transverse mode spacing

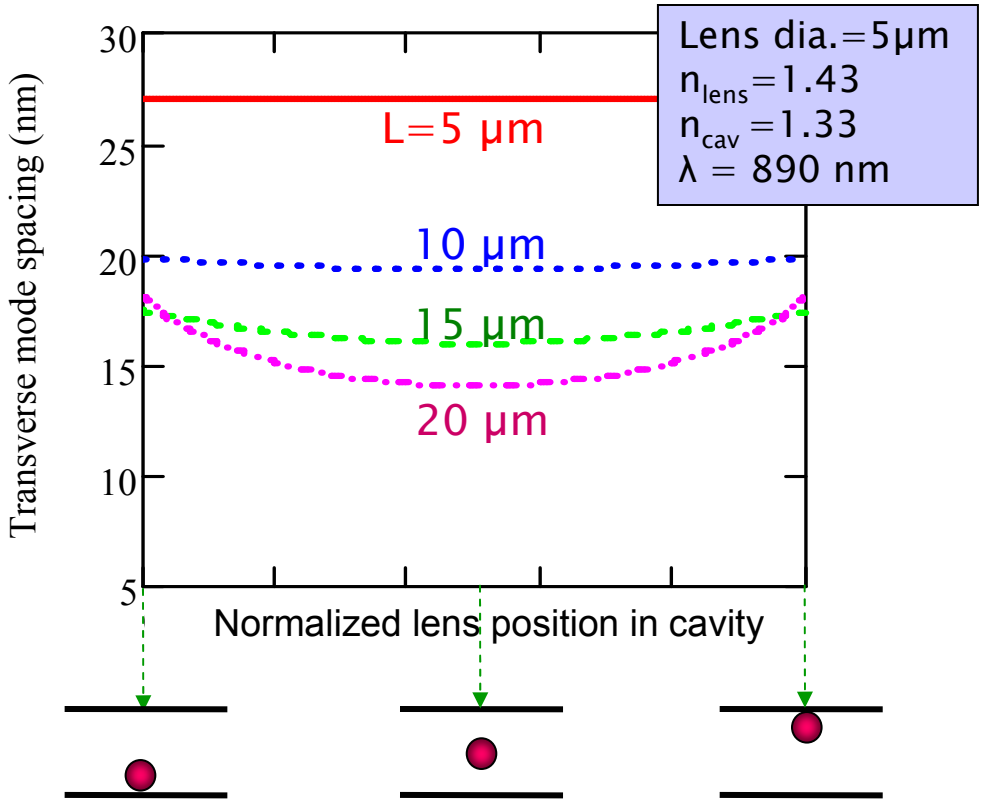

Conclusions

- The cavity length should be minimized in order to provide stable resonator operation for sphere positions throughout the resonator and to reduce the shift in frequencies with sphere position.

Double sphere model for a cell

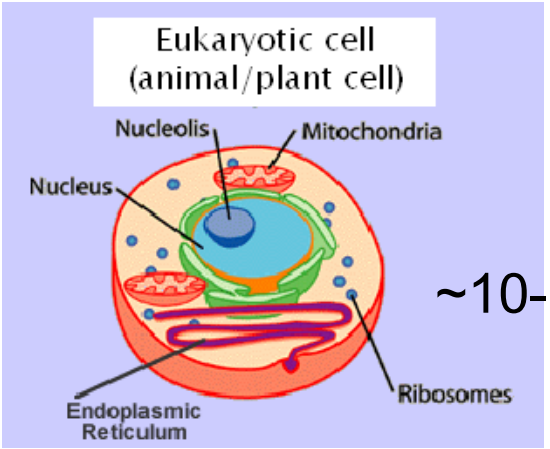

~10-100 μm

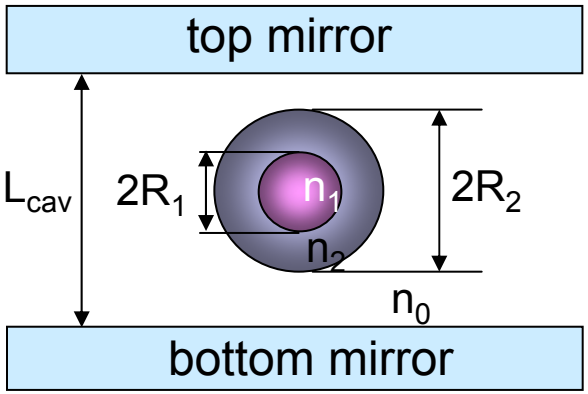

Reported values

n_0 : RI of cavity media (1.33~1.35)

n_1 : RI of cell nucleus (1.4~1.6)

n_2 : RI of cytoplasm (1.35~1.36)

$2R_1$: Diameter of nuclei of lymphocytes (~7 μm)

$2R_2$: Diameter of lymphocytes (8~15μm)

Double homogeneous sphere model has been widely used for cells in scattering spectroscopy.

Effective index method

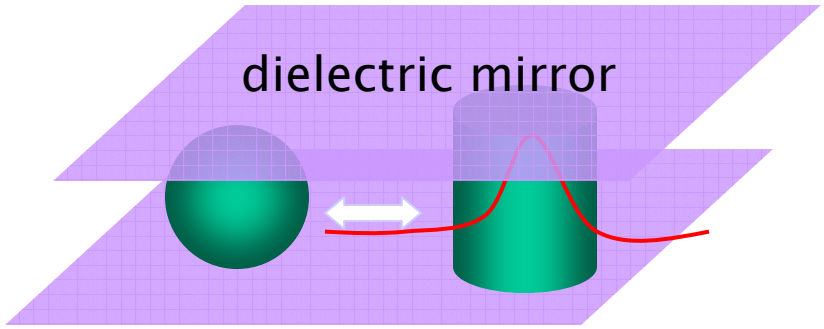

$$\frac{\Delta n_{eff}}{n_{eff}} = \frac{\Delta \lambda}{\lambda}$$

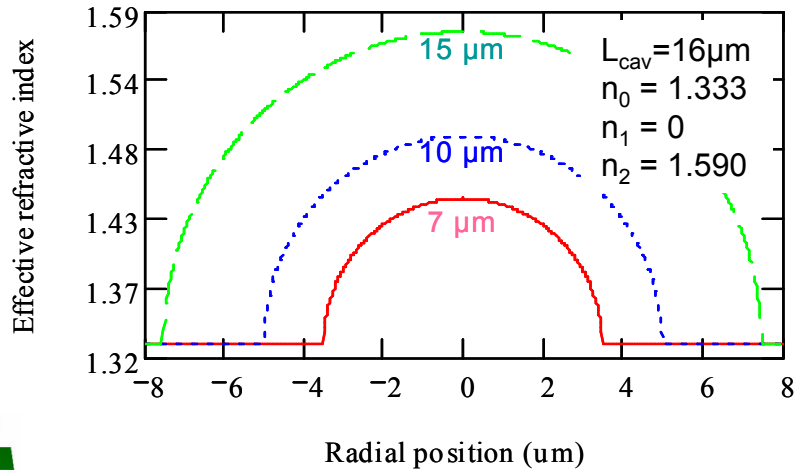

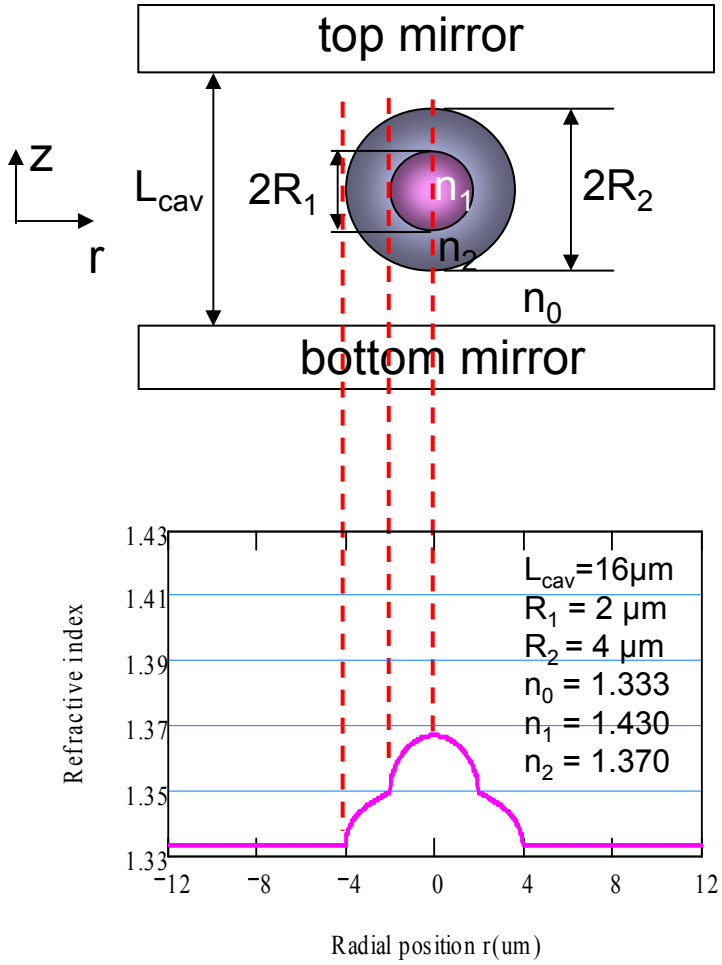

Numerical mode solver

$$\nabla^2 E + \nabla\left(\frac{\nabla \varepsilon_r}{\varepsilon_r}\cdot E\right) + k_0^2 \varepsilon_r E = 0 \quad \Leftarrow \quad E_t(r,\phi,z) = V(r) e^{iv\phi} e^{i(\omega t - \beta z)}$$

$$\frac{d^2}{dr^2}V(r) + \frac{1}{r}\frac{d}{dr}V(r) + \frac{d}{dr}\left[\frac{1}{\varepsilon(r)}\left(\frac{d}{dr}\varepsilon(r)\cdot V(r)\right)\right] + \left(k_0^2\varepsilon(r) - \beta^2 - \frac{v^2}{r^2}\right)\cdot V(r) = 0$$

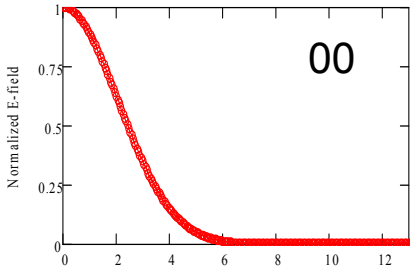

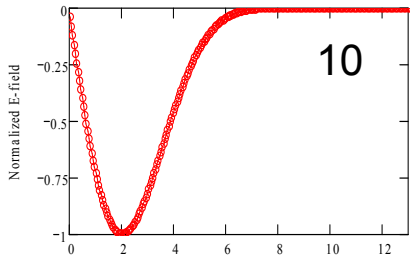

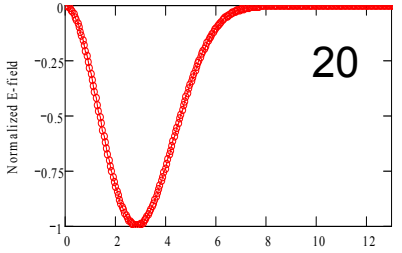

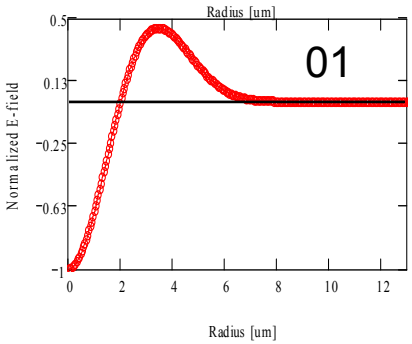

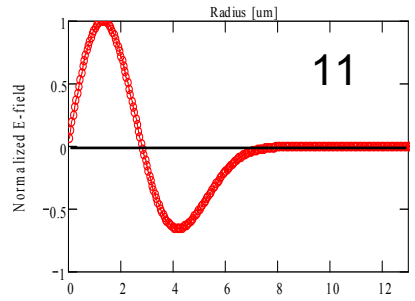

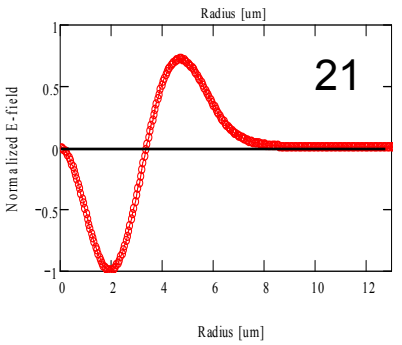

$n_{cav} < n_{eff} < n_{max}$

Modeling vs. experiment

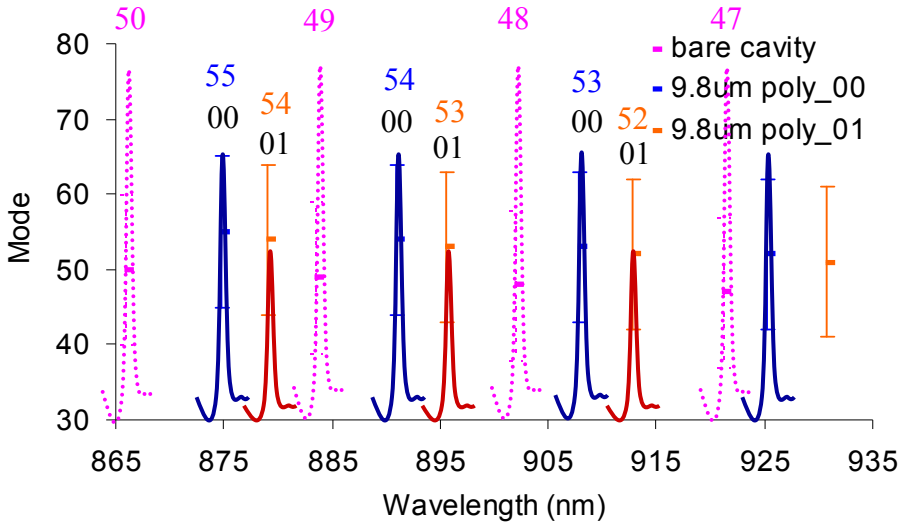

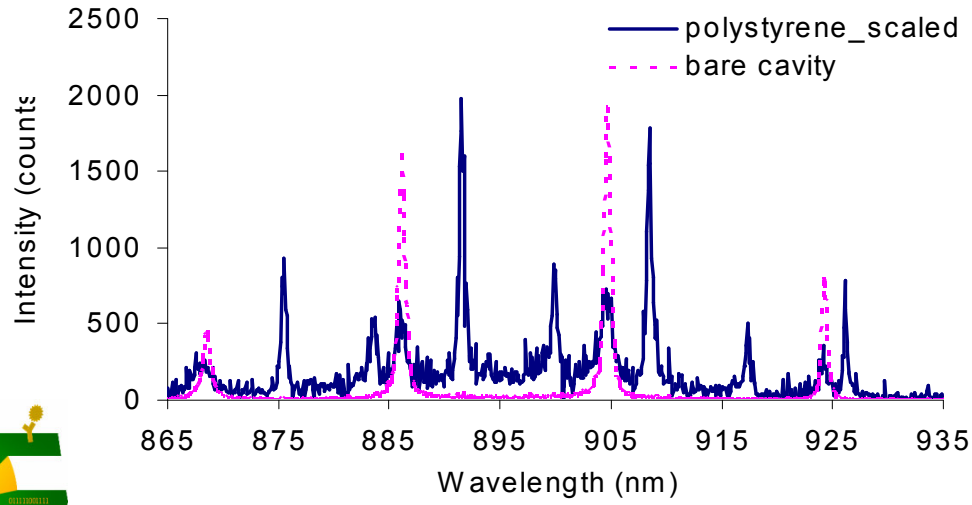

Modeling parameters:

- n=1.59 (polystyrene)
- D_{sphere}=9.77±0.85 μm
- DI water (n=1.330)
- Mode hops to the long wavelength side by 5 groups

Mode position vs. sphere size variation

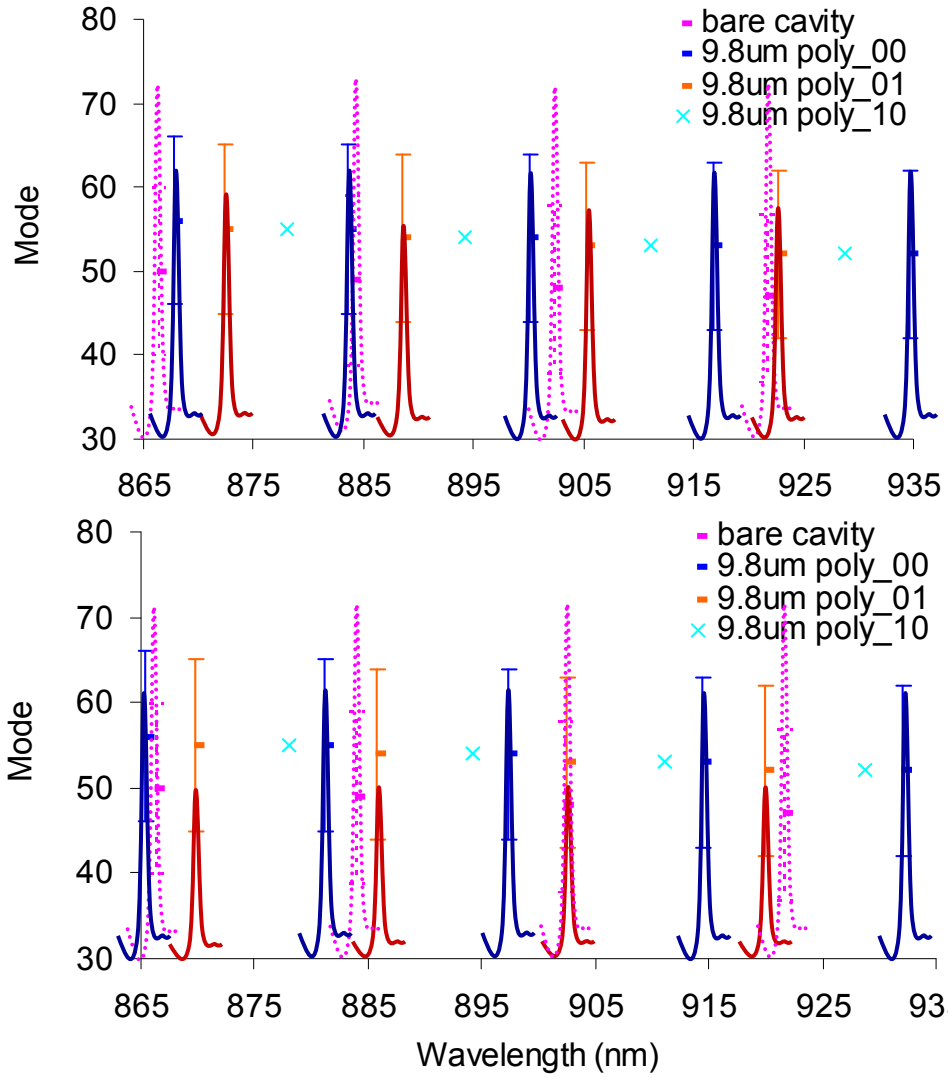

D_{sphere}=9.77+0.85 μm

D_{sphere}=9.77+0.6 μm

Sphere with small size variation

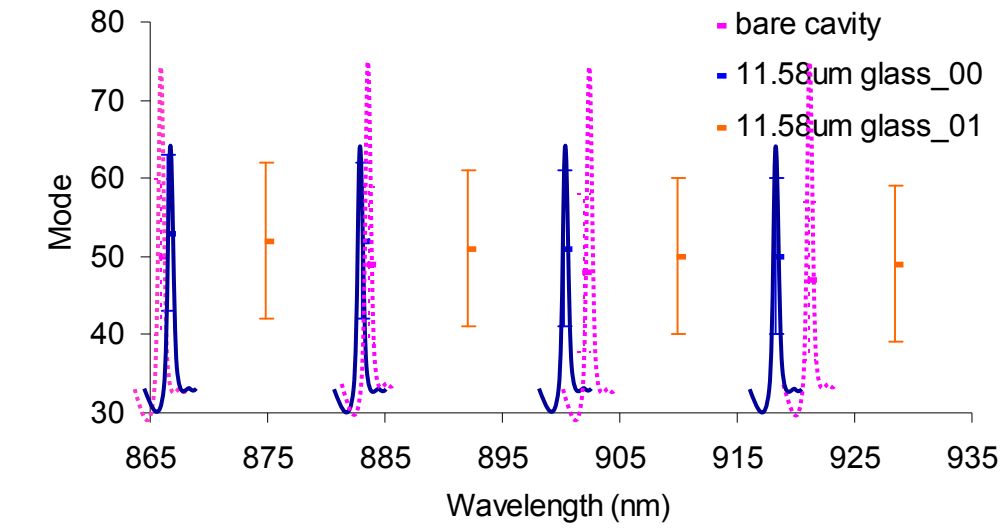

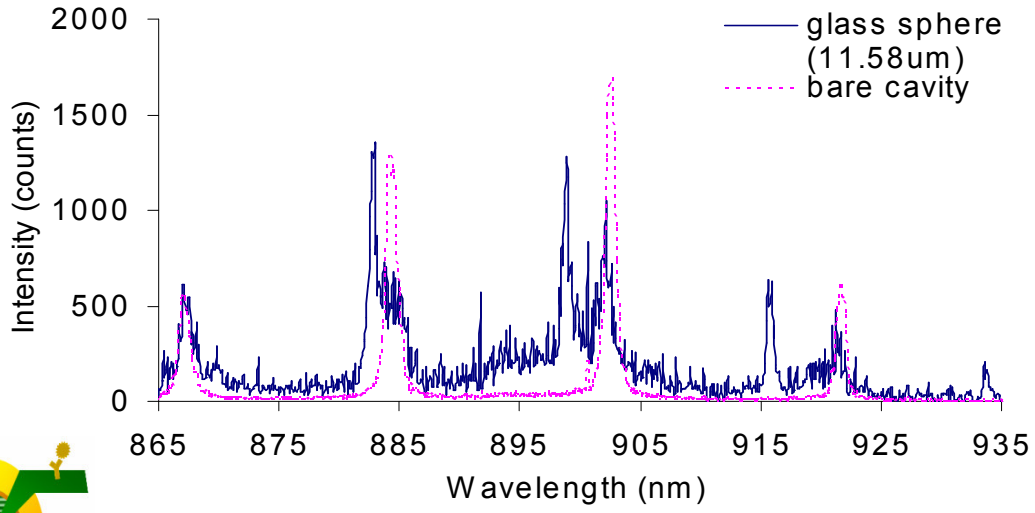

Modeling parameters

- n=1.45 (glass microspheres)
- D_{sphere}=11.58±0.19 μm
- DI water (n=1.330)
- Mode hopes to long wavelength side by 2

PBS refractive index measurement

$$m\lambda_{n1} = 2n_1 L_{cav} \qquad m\lambda_{n2} = 2n_2 L_{cav}$$

$$\frac{n_{PBS}}{n_{DI\_water}} = \frac{\lambda_{n2}}{\lambda_{n1}}$$

1.330 @ 25^{0}C and 890nm

$dn_{DI\_water}/dt = -0.00009$ per ^{0}C

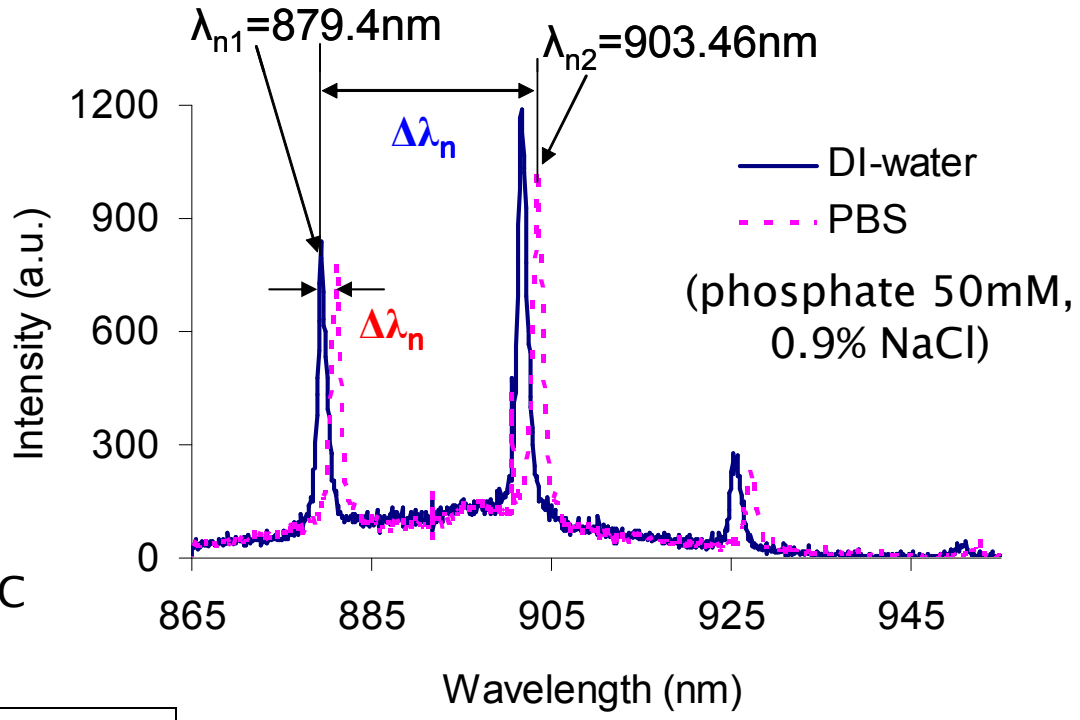

Other publication reports

n_{PBS}=1.3342

(phosphate 69mM, NaCl 150mM, pH 7.6)

Without mode hop : n_{PBS}=1.333

With mode hop : n_{PBS}=1.363 ??

Nuclear RI calculation for lymphocytes

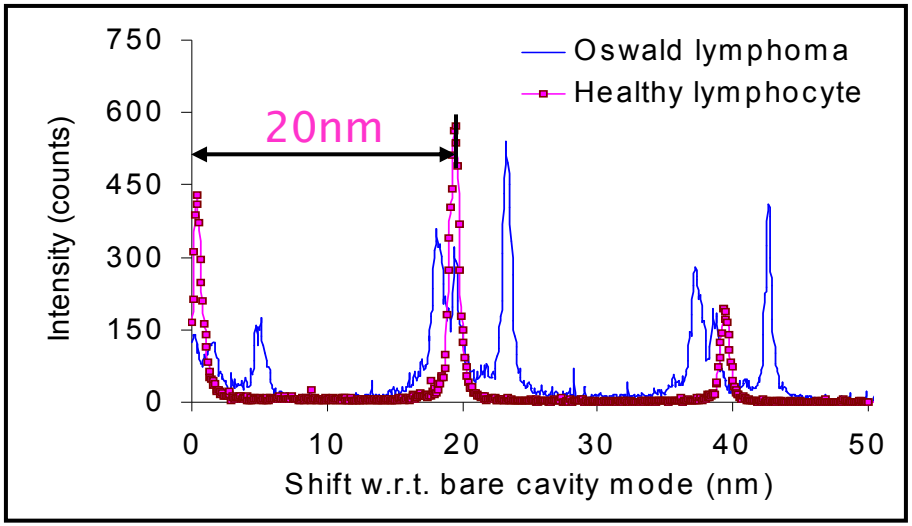

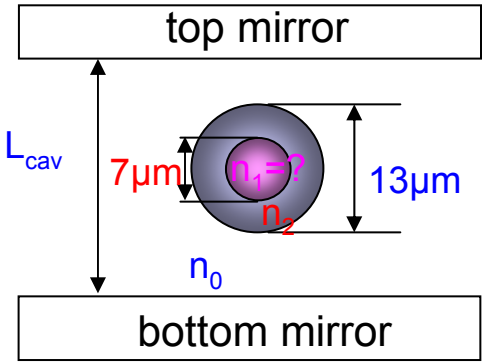

- $\Delta\lambda$=20.18nm → effective RI of lymphocyte mode, n^*=1.375
  - Ambiguity in mode order resolved by reference to range of published values
- Microscopic size measurement → cell diameter is 13 μm

Assumptions made based on published data:

- Nuclear diameter is 7 μm (nucleus-to-cytoplasm volume ratio is approximately 1:5 for normal cells)
- Cytoplasmic RI : n_2=1.350

2D mode solver ⇒ $n_{nucleus}$=1.3987

Optical model for lymphoma

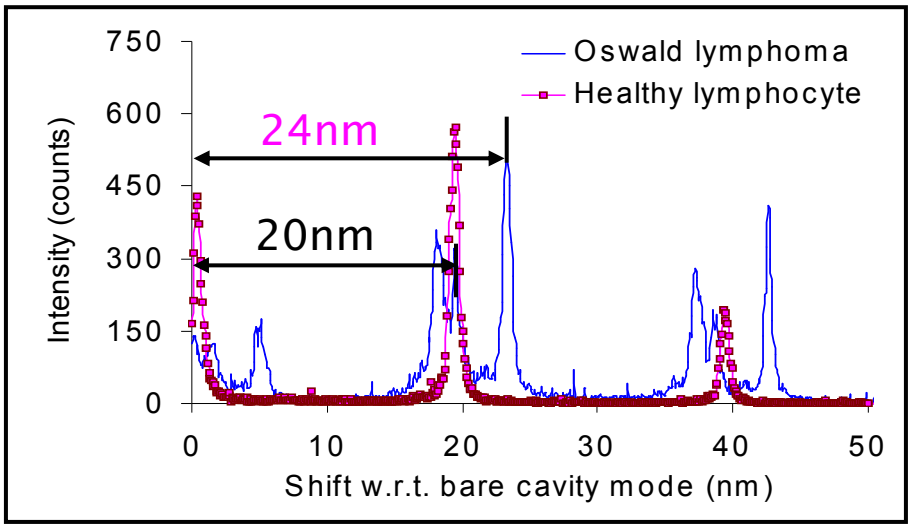

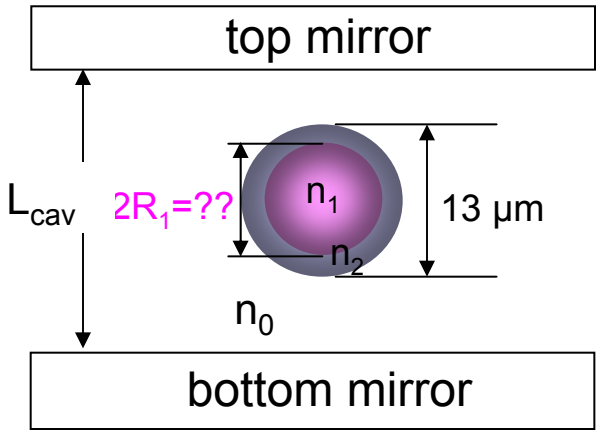

- n_1=1.399 (same as for lymphocyte) and n_2=1.350
- $\Delta\lambda_{cytoplasm}$ = 20.363 ± 0.404 nm (nearly same as lymphocytes)
- $\Delta\lambda_{nucleus}$ = 24.593 ± 0.127 nm

2D mode solver ⇒ $R_1 = R_{nucleus} =$ 4.457 μm

Comparison with 1-D model

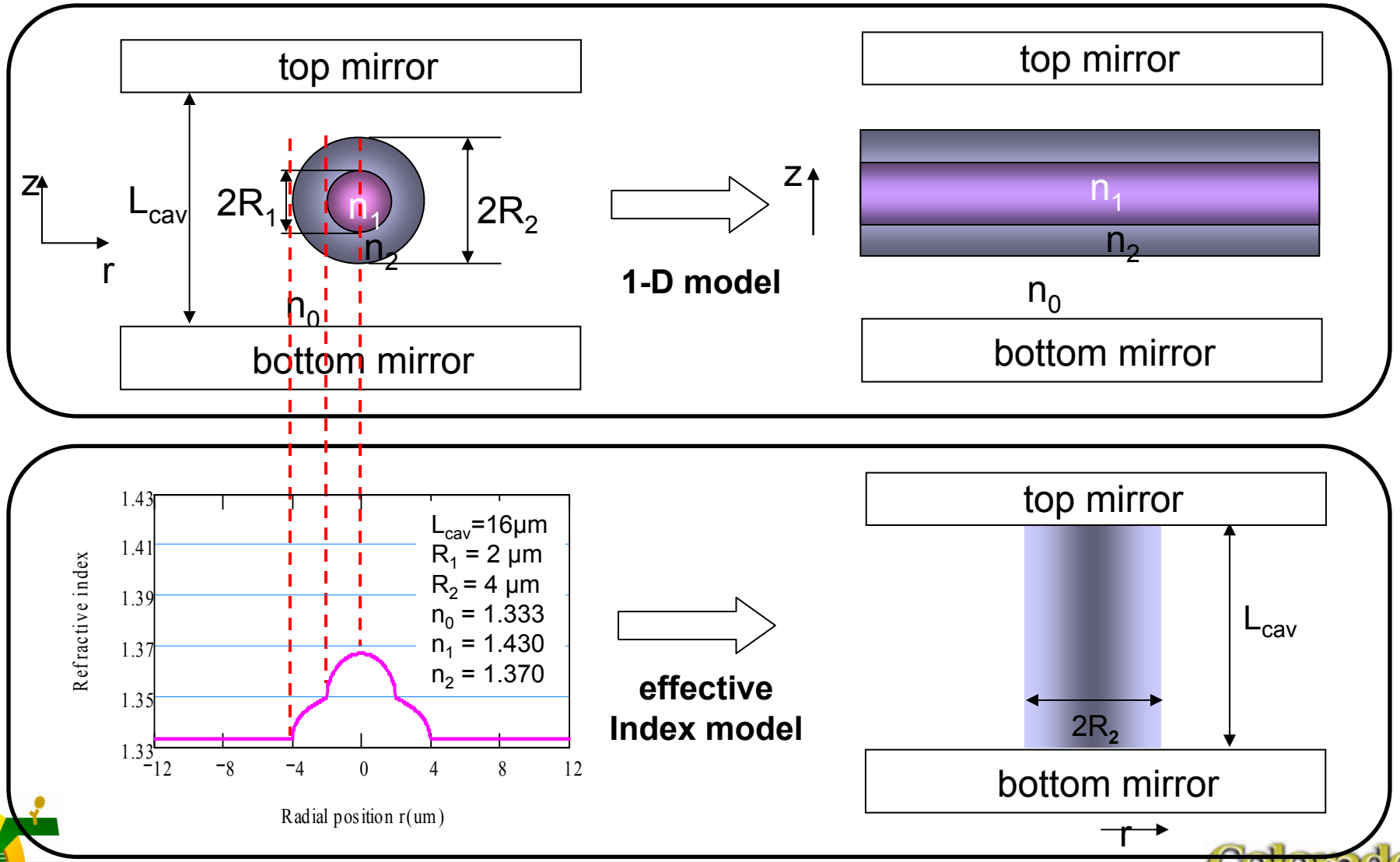

Nuclear mode shift vs. size and RI

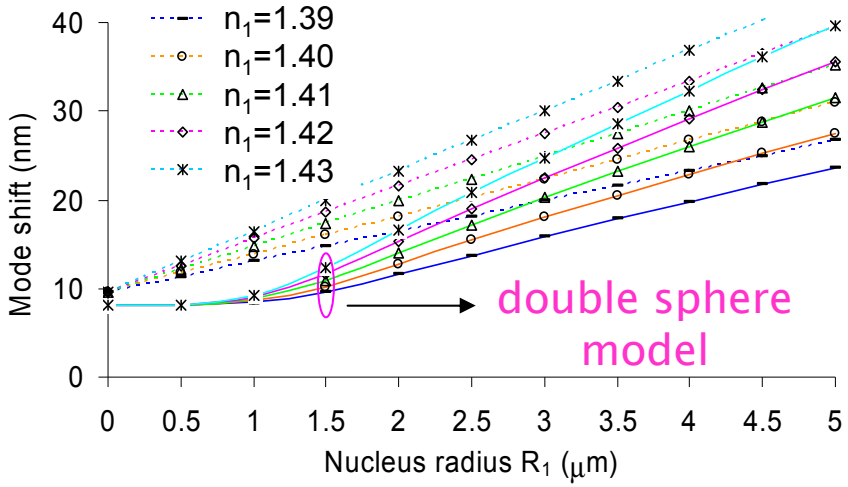

Transverse mode confinement effects are important for correctly interpreting mode shifts.

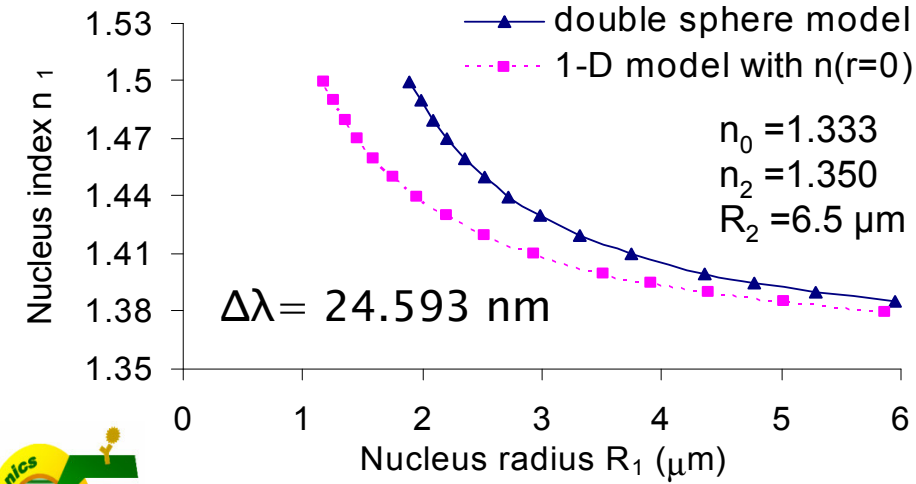

The double sphere model offers an improved estimate of nuclear RI, especially for cells with a small nucleus.

Rsoft Fullwave FDTD simulation

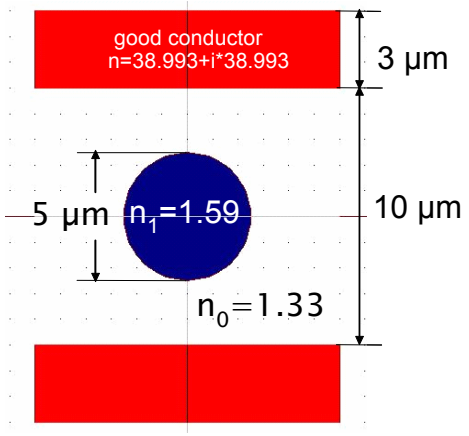

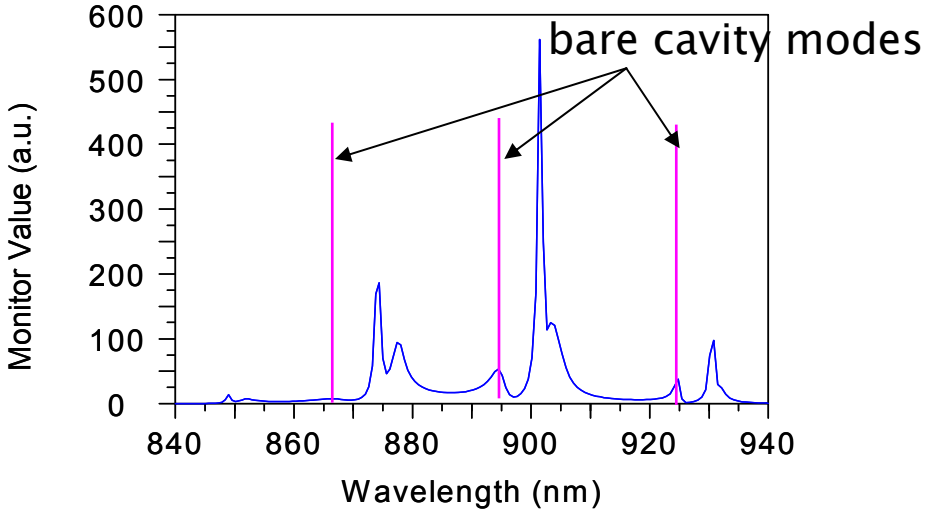

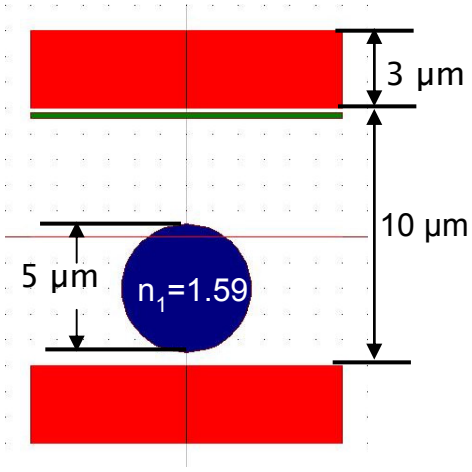

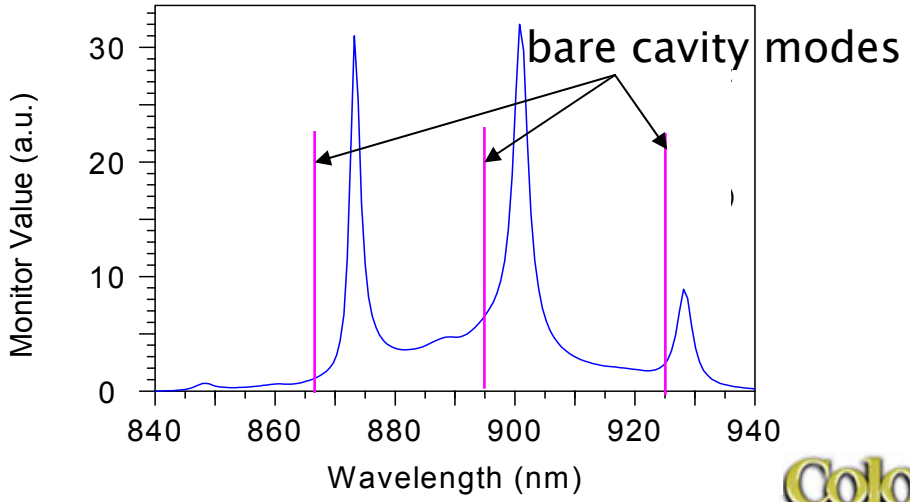

Lumerical FDTD simulation

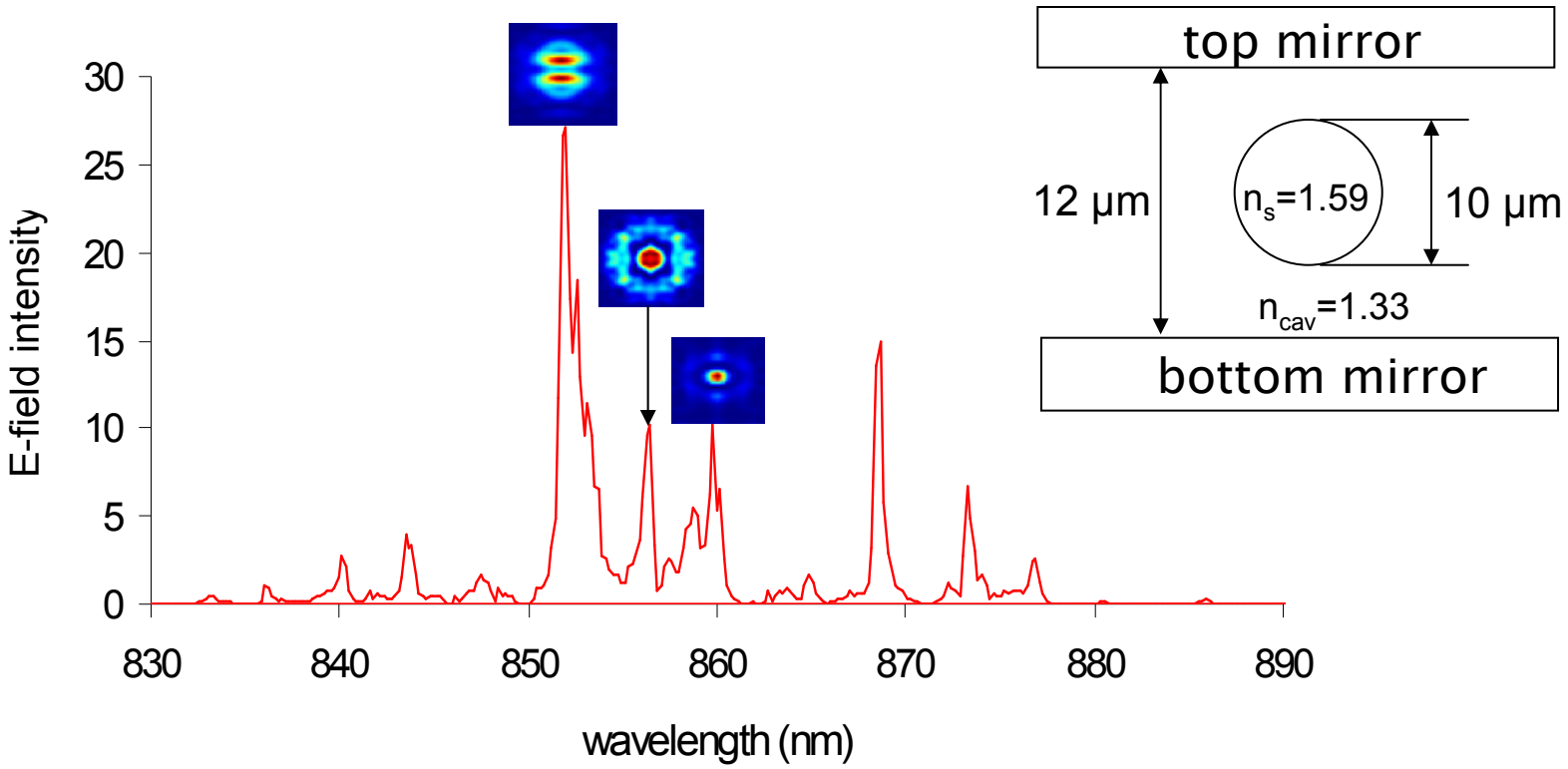

It takes 28 hours to run one simulation on a 2.4GHz Pentium IV computer with 768MB RAM.

Summary

- Developed complete fabrication processes for OFIS cavities.
- Characterized the optical cavity finesse experimentally and theoretically.
- Measured transmission spectra of different types of biological cells and microspheres.
- Identified the order of each modes experimentally and verified with the numerical modeling.
- Developed simplified optical models to simulate the spectra of sphere and cell loaded OFIS cavities.

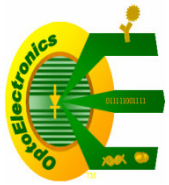

Colorado State University

Published and submitted papers

- Journal papers

1. H. Shao, W. N. Wang, S. E. Lana, and K. L. Lear, "Optofluidic intracavity spectroscopy of canine lymphoma and lymphocytes", submitted to *IEEE Photonics Technology Letters*, July 2007, in revision.

2. H. Shao, D. Kumar, and K. L. Lear, "Single cell detection using optofluidic intracavity spectroscopy", *IEEE Sensors Journal*, 6(6), 1543-1550, 2006.

3. H. Shao, D. Kumar, S. A. Feld, and K. L. Lear, "Fabrication of a Fabry-Pérot cavity in a microfluidic channel using thermocompressive gold bonding of glass substrates", *IEEE Journal of MEMS*, 14(4), 756-762, 2005.

Published and submitted papers

- Conference presentations

1. H. Shao, W. N. Wang, S. E. Lana and K. L. Lear, APS Annual Meeting, paper B38.00006, Denver, Colorado, March 5, 2007.
2. H. Shao and K. L. Lear, IEEE LEOS 19th Annual Meeting, Montreal, Canada, October 30, 2006.
3. H. Shao, S. E. Lana, and K. L. Lear, IEEE LEOS 19th Annual Meeting, Montreal, Canada. October 30, 2006.
4. H. Shao, D. Kumar, and K. L. Lear, IEEE LEOS Summer Topicals-Optofluidics, Quebec City, Canada, July 17, 2006.
5. H. Shao, D. Kumar, and K. L. Lear, 14th IEEE Sensors Conference, Irvine, California, October 31, 2005.
6. H. Shao, D. Kumar, and K. L. Lear, CLEO/QELS, Baltimore, Maryland, May 22, 2005.
7. H. Shao, D. Kumar, S. A. Feld and K. L. Lear, IEEE LEOS 17th Annual Meeting, vol. 1, pp. 120-121, Puerto Rico, November 7, 2004.
8. H. Shao, D. Kumar and K. L. Lear, the 49th Annual SPIE Conference, Denver, August 4, 2004.

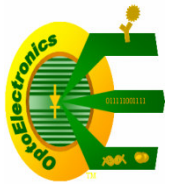

Colorado State University

Acknowledgement

- Dr. Menoni, Dr. Chandrasekar, and Dr. Henry, committee members
- Dr. Lear, research advisor
- Optoe group members
- Dr. Lana, B. Rose, and A. Cunkelman, collaborators at the CSU veterinary hospital
- Anonymous journal paper reviewers

Thank you!

Questions?

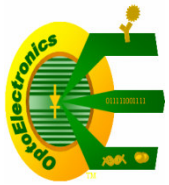

Colorado State University